

## FEATURE ARTICLE

## Magnetic Isotope Effect: Nuclear Spin Control of Chemical Reactions

Anatoly L. Buchachenko\*

*N.N. Semenov Institute of Chemical Physics, Moscow 117334 Russia**Received: April 4, 2001; In Final Form: July 25, 2001*

Molecular transformation (chemical reaction) as an electron–nuclear rearrangement of the reactants into the products is the heart of chemistry, the central event which all chemistry circulates about. It is selective to the nuclei, both in mass and spin. Nuclear mass selectivity of reactions results in classical isotope effect (CIE), the remarkable phenomenon which continues to play a unique role and has served served for many years as a powerful and reliable tool of mechanistic chemistry and biochemistry. Another breakthrough of similar scale and importance is the discovery of nuclear spin selectivity of chemical reactions, which is the dependence of the reaction rates on the nuclear spin and nuclear magnetic moment of the reactants. In contrast to CIE, which is governed by chemical energy of the starting and transition states of reactant molecules, this new isotope effect is controlled by magnetic interactions, so it was christened the magnetic isotope effect (MIE). The general principles of tuning of the reactions to MIE are discussed, particularly by microwaves, tunable on frequency and amplitude, to selectively modify and control chemical reactivity.

## MIE Is a Highlight in Spin Chemistry

**A. Spin Chemistry as a New Chemical Land.** In a recent brilliant feature article,<sup>1</sup> Ahmed H. Zewail has presented a striking and impressive overview of the new frontier in modern chemistry—femtochemistry, which explores atomic motions on the potential energy surface, vibrational and rotational coherence of the wave packets, and transition state spectra, geometry, and dynamics. Another new frontier is spin chemistry, which monitors the behavior of angular momentum (spin) of electrons and nuclei in chemical reactions (including coherence of spin wave packets), spin dynamics and spin state evolution of reactants, chemical generation, and reception of microwaves;<sup>2</sup> the latter is a subject of chemical radiophysics, a part of spin chemistry.

Spin chemistry is based on the fundamental and universal principle of spin conservation: all chemical reactions are spin-selective, they allowed only for those spin states of reactants whose total spin is identical to that of products. Spin chemistry

is unique: it introduces in chemistry magnetic interactions. Contributing almost nothing in chemical energy, being negligibly small and traditionally ignorable, magnetic interactions are the only ones which are able to change electron spin of reactants and switch over the reaction between spin-allowed and spin-forbidden channels. Ultimately, they control chemical reactivity and write a new, magnetic scenario of chemical reaction.

**B. Magnetic Effects in Chemical Reactions.** All scenes of the magnetic play performed by chemical reaction may be illustrated by the radical pair, which plays in spin chemistry a testifying role similar to that of the H<sub>2</sub> molecule in quantum chemistry.

Suppose that there is a triplet radical pair (R••R) prepared by photolysis, by radiolysis, or by encounter of freely diffusing radicals (Figure 1). To recombine and produce diamagnetic, zero-spin molecule RR, triplet–singlet spin conversion of the pair is required. This is a culminating phase of the spin-selective recombination reaction, and it has nothing to do with chemistry because spin conversion is induced by physical, magnetic forces.

\* E-mail: spinchem@chph.ras.ru.

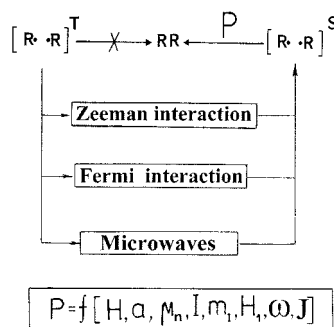


**Figure 1.** General scheme of spin conversion induced by Zeeman and Fermi interactions and microwaves. Radical pair functions as a spin-selective nanoreactor in which the reaction probability  $P$  is a function of magnetic parameters of the radicals ( $a$ ,  $\mu_n$ ,  $I_n$ ,  $m_l$ ), magnetic fields ( $H$ ,  $H_1$ ,  $\omega$ ), and exchange interaction  $J$ .

Three of them are the most important characters of the magnetic scenario: the electron Zeeman interaction, the electron–nuclear Fermi interaction (well-known in ESR spectroscopy as a hyperfine coupling), and microwaves. By spin changing, they transform nonreactive triplet state of the pair into the reactive singlet state (triplet–singlet conversion), so the reaction probability in the radical pair ( $R\cdot R$ ) is a function of all parameters characterizing these magnetic interactions:

$$P = f[H, a, \mu_n, I, m_l, H_1, \omega, J] \quad (1)$$

It is a function of the magnetic field  $H$ , the nuclear spin  $I$  and its projection  $m_l$ , the nuclear magnetic moment  $\mu_n$ , the hyperfine electron–nuclear coupling constant  $a$ , the frequency  $\omega$  and amplitude  $H_1$  of the microwave magnetic field, and the exchange interaction  $J$  between unpaired electrons of the radical partners. Evidently, a radical pair functions as an electron and nuclear spin-selective chemical microreactor.<sup>3</sup>

Function 1, like a horn of plenty, generates all remarkable phenomena in spin chemistry:

- (i) magnetic field effect
- (ii) chemically induced electron and nuclear polarization (CIDEP and CIDNP)
- (iii) chemically detected magnetic resonance
- (iv) microwave emission (chemical maser)
- (v) spin catalysis
- (vi) magnetic isotope effect
- (vii) microwave magnetic isotope effect
- (viii) microwave stimulated nuclear polarization
- (ix) spin coherency in chemical reactivity
- (x) single-spin tunneling spectroscopy

As a spin-selective microreactor, a radical pair is not unique. A pair of any spin carriers (radicals, paramagnetic ions and carbenes, triplet and high-spin molecules, solvated or trapped electrons, paramagnetic holes, vacancies and dislocations in solids, etc.) is a multispin system with a manifold of spin states. Chemical reaction selects those of them which are spin-allowed; spin-forbidden states undergo magnetically induced spin conversion, so any multispin pair is a spin-selective microreactor and a potential source of magnetic effects.

For example, chemical addition of radical to triplet molecule (oxygen, for instance), as well as physical quenching of excited triplet molecule by radical, results in products in doublet spin state. But their precursor is a three-spin pair of reactants with spin-allowed doublet D and spin-forbidden quartet Q spin states. Magnetic interactions stimulate quartet–doublet spin conversion and open an additional reaction channel responsible for the magnetic effect in this D + T reaction.

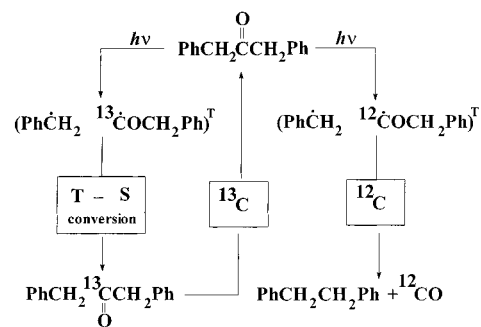


**Figure 2.** Scheme of MIE-induced isotope fractionation in the photolysis of dibenzyl ketone.

Similarly, in the reaction of two triplets (recombination of triplet carbenes, addition of oxygen to triplet molecule, delayed fluorescence from annihilation of two triplets, etc.), only one of the nine available spin states of the (T T) pair is able to react; however, spin conversion of the others driven by magnetic interactions provokes magnetic effects in this T + T reaction. Chemical manifestations of the effects in D + T and T + T reactions will be given later.

**C. Why MIE is a Highlight.** The majority of magnetic effects listed above are now assimilated in powerful experimental techniques which are widely used to probe the reaction intermediates and to investigate reaction mechanisms both in chemistry and biochemistry (for instance, magnetic field effect in enzyme processes,<sup>4</sup> microwave studies of photosynthetic center,<sup>5</sup> magnetic and microwave effects in dislocation mobility and micromechanics of solids,<sup>6</sup> etc.). Unlike others, MIE is much more than simply an experimental technique and a powerful tool of mechanistic chemistry (see section 6).

MIE is the most chemically significant phenomenon, substantially contributing in chemistry and related sciences (geochemistry, space chemistry, life science). It is a phenomenon of fundamental importance. As a powerful mechanism of isotope fractionation MIE should be taken into account, in conjunction with CIE, to accurately reconstruct genesis and pathways of chemical evolution of matter and of its components (minerals, oils, ores, coals, interstellar substances, etc.). Any isotope anomalies and deviations in isotope composition trace chemical history of the nature.

MIE bears new ideas how to control chemical reactions by spin manipulation. Chemistry is generally known to be controlled by two “tyrants”, energy and angular momentum (spin).<sup>7</sup> For the long history of chemistry, the energy control has been advanced, if not perfectly then quite successfully; however, an era of spin control is only forthcoming and MIE is expected to be one of the cornerstone in progress of chemistry along this way.

**D. MIE: How It Functions.** MIE is a purely kinetic phenomenon, the dependence of the reaction rate (rate constant, reaction probability) on the nuclear spin and nuclear magnetic moment of the reactants. In contrast to CIE, which selects isotopic nuclei according to their mass, MIE separates isotopes by spin and magnetic moment. Figure 2 demonstrates how MIE functions and how MIE-induced isotope fractionation occurs.

Photolysis of dibenzyl ketone (DBK) is known to proceed by fragmentation of excited molecule in triplet state into the triplet pair of acyl and benzyl radicals. Starting from this point, the fate of the pair depends on whether it carries magnetic (<sup>13</sup>C) or nonmagnetic (<sup>12</sup>C) nuclei. The “magnetic” radical pair (with, suppose, <sup>13</sup>C in carbonyl position) undergoes fast triplet–singlet conversion, induced by hyperfine coupling between unpaired electron and magnetic nucleus <sup>13</sup>C (its energy about 125 G, or

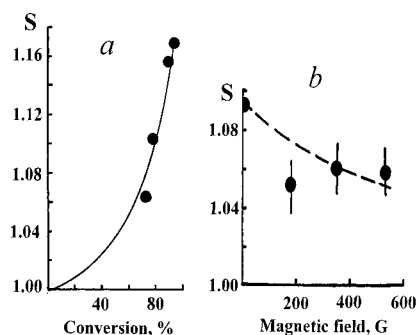


**Figure 3.**  $^{13}\text{C}$  isotope enrichment  $S$  of dibenzyl ketone as a function of chemical conversion (a) and magnetic field (b).

$1.2 \cdot 10^{-5}$  eV), and recombine regenerating starting DBK molecule. Triplet–singlet conversion of “nonmagnetic” pair (with  $^{12}\text{C}$  in carbonyl group) is strongly delayed since only protons contribute into the hyperfine coupling (its total energy is 5-fold lower than that in magnetic pair), so the nonmagnetic pair predominantly dissociates and results in reaction products (dibenzyl and carbon monoxide). Thus, due to the difference in the rates of spin conversion, the radical pair sorts the nuclei and dispatches magnetic and nonmagnetic nuclei into different reaction products: regenerated ketone accumulates  $^{13}\text{C}$ , and carbon monoxide collects  $^{12}\text{C}$ .

The discovery of MIE in 1976<sup>8</sup> in the photolysis of DBK made this reaction famous and popular; physical chemistry and physical and kinetic theories of MIE are tested mostly by this reaction.

## 2. MIE: The Road of Discoveries

After the observation of chemically induced polarization of protons in radical reactions<sup>9</sup> (CIDNP phenomenon), it was deliberated that these reactions are nuclear spin-selective; i.e., their rates depend on the nuclear orientation and, probably, should depend on the nuclear spin itself. Lawler and Evans<sup>10</sup> were the first who reported this idea. However, the possibility to observe nuclear spin dependence of the reaction rates was not evident: CIDNP has clearly demonstrated that the acceleration of reaction for some spin orientations is compensated by deceleration for opposite spin orientations since the populations of Zeeman nuclear spin states are identical (with accuracy of  $10^{-6}$ ). The sorting of nuclear spin orientations does not imply the sorting of nuclear spin themselves; for this reason, the pure nuclear spin effect was expected to be negligible and hardly detectable.

The first observation of the enormously large  $^{13}\text{C}$  nuclear polarization<sup>11</sup> in the reactions of peroxides has inspired target-oriented hunting for  $^{13}\text{C}$  nuclear spin effect on reaction rates.

**A. Carbon-13 MIE.** The discovery of the new, nuclear spin isotope effect was announced in 1976<sup>8</sup> in the paper entitled “Isotope Enrichment Induced by Magnetic Interactions in Chemical Reactions”. In the photodecomposition of dibenzyl ketone (DBK) at 20 °C in benzene, isotope enrichment of DBK by  $^{13}\text{C}$  was shown to strongly increase as the chemical conversion of DBK increases (Figure 3a). It is hardly disputable that the classical isotope effect is not able to ensure such a huge effect; even more convincing was the magnetic field dependence of the effect (Figure 3b), which is the direct evidence of its magnetic nature (on this basis, the new effect was christened the magnetic isotope effect by Buchachenko).

The year 1976 gave a start for the race in search for MIE. Next year Sagdeev et al. have announced the discovery of MIE in triplet sensitized photolysis of benzoyl peroxide: the reaction

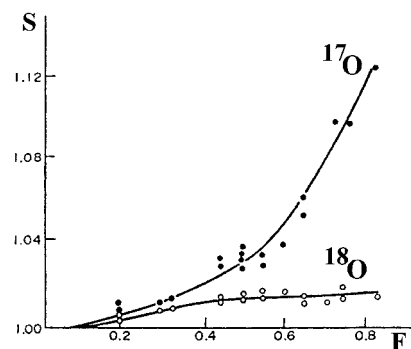
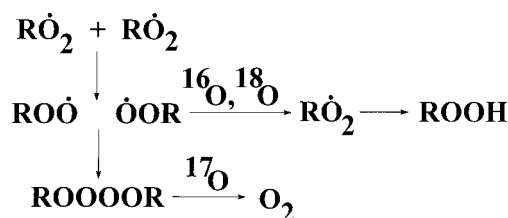


**Figure 4.** Oxygen MIE and isotope enrichment  $S$  of molecular oxygen in the chain termination reaction of polymer oxidation as a function of chemical conversion  $F$  of oxygen.

product, phenyl benzoate, was  $^{13}\text{C}$  enriched by  $\sim 6\%$ .<sup>12</sup> Two years later, in 1978, Turro et al. confirmed MIE in the DBK photolysis in micelles.<sup>13</sup> Turro was the first who used micelles as microreactors for the photolysis reactions; he has shown that the reactions in micelles result in strong enhancement of MIE induced isotope separation.<sup>14</sup> In 1980, Pines and co-workers showed that in viscous solutions (in cyclohexanol, for instance) MIE in DBK photolysis markedly increases.<sup>15</sup> An even larger effect (higher than in micelles) was detected in 1980 by Tarasov et al. in DBK photolysis in very viscous mixtures of glycerol and tertbutanol (see section 5). In 1980, Tarasov and Buchachenko, besides DBK enrichment, studied isotope impoverishment of  $\text{PhCH}_2\text{CH}_2\text{Ph}$ , a product of DBK photolysis, and completed a total isotope balance on the different isotope forms of DBK molecule (section 5).<sup>16</sup> Later, MIE was found in the photolysis of DBK on porous silica and zeolites<sup>17</sup> and in the photolysis of phenyl adamantyl ketone<sup>18</sup> and many others, including cyclic ketones.<sup>19</sup> Temperature<sup>20</sup> and wavelength effects<sup>21</sup> on the MIE in the photolysis of ketones have also been studied (section 5).

**B. Oxygen-17 MIE.**  $^{17}\text{O}$  MIE was seen in 1978<sup>22</sup> in the liquid-phase oxidation of ethylbenzene by molecular oxygen; the latter was shown to be enormously enriched by  $^{17}\text{O}$  with respect to that by  $^{18}\text{O}$ . Later, the extensive studies of MIE in chain oxidation processes of hydrocarbons (ethylbenzene, isopropylbenzene) and polymers (polyethylene, polypropylene, polymethylpentene, polyisobutylene, natural rubber, polyoxides and others) have discriminated two spin-selective and isotope-sorting reactions—recombination of peroxyradicals and addition of alkyl radicals to dioxygen; the former dominates in polymer oxidation and the latter prevails in liquid-phase oxidation of hydrocarbons and polymers in solutions.<sup>23</sup>

The scheme of isotope sorting in the chain termination reaction is shown in Figure 4. The encounter pair of freely diffusing peroxy radicals is a spin-selective nanoreactor: it dispatches different nuclei into the different products. The ratio of singlet and triplet spin state populations in these pairs is 1:3, but, being negligibly small in singlet pairs (they mostly react almost instantly), MIE arises in the triplet–singlet spin conversion of the long living triplet pairs. Because of MIE, the recombination probability of peroxy radicals with terminal

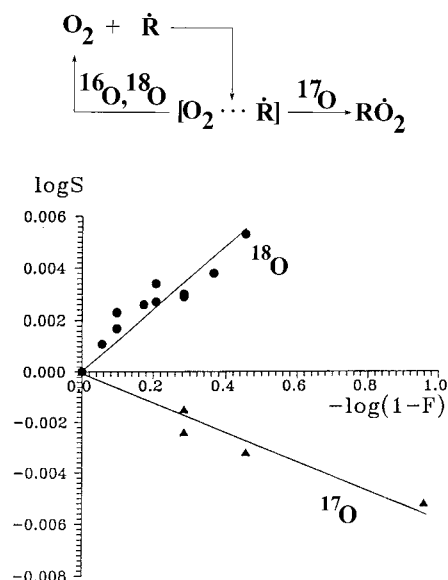


**Figure 5.** Oxygen isotope enrichment  $S$  in the chain propagation reaction of ethylbenzene oxidation by molecular oxygen as a function of chemical conversion.

magnetic  $^{17}\text{O}$  nuclei is higher than that of radicals with nonmagnetic  $^{16}\text{O}$  and  $^{18}\text{O}$  nuclei. As a result, peroxy radicals carrying  $^{17}\text{O}$  nuclei predominantly recombine into the unstable tetraoxide, which decomposes regenerating molecular oxygen enriched by  $^{17}\text{O}$ , while the hydroperoxide molecules lose these nuclei. Figure 4 demonstrates the isotope enrichment of dioxygen as a function of its conversion: the higher chemical conversion results in higher isotope enrichment.

By analysis of these dependences for the oxidation of polymers, the ratio of the rate constants of the chain termination reaction was found:

$$k(\text{RO}^{17}\text{O}^{\bullet})/k(\text{RO}^{16}\text{O}^{\bullet}) = 1.8 \pm 0.1$$

i.e., the substitution of nonmagnetic nucleus  $^{16}\text{O}$  by magnetic one  $^{17}\text{O}$  almost doubles the rate constant of radical recombination; this ratio does not depend on the chemical structure of the alkyl radical  $\text{R}$ .

In contrast to oxidation of solid polymers, liquid-phase oxidation is accompanied by impoverishment of the recovered molecular oxygen by  $^{17}\text{O}$  nuclei.<sup>23c</sup> The opposite sign of MIE certainly eliminates termination reactions as a main source of isotope selection. It has been concluded that another spin-selective chain propagation reaction, the addition of alkyl radical to molecular oxygen (Figure 5), plays a dominant role in the nuclear sorting. In this case, a spin-selective nanoreactor is the encounter three-spin pair ( $\text{R}^{\bullet}\cdots\text{O}_2$ ) in doublet or quartet spin states in a ratio of 1:2. Again, doublet states react almost instantly, without significant doublet-quartet spin evolution, while quartet states undergo nuclear spin dependent quartet-doublet conversion. Because of hyperfine coupling in  $^{17}\text{O}^{16}\text{O}$ , the pairs carrying these oxygen molecules experience fast spin conversion and react faster than those with  $^{16}\text{O}_2$  or  $^{18}\text{O}^{16}\text{O}$  molecules. As a result, molecular oxygen as a reactant loses magnetic  $^{17}\text{O}$  nuclei. In contrast, oxygen molecules with  $^{18}\text{O}$  react slower than those with  $^{16}\text{O}$  resulting slightly in the CIE-induced enrichment of molecular oxygen by  $^{18}\text{O}$ .

Figure 5 depicts the typical dependence of isotope enrichment  $S$  on the oxygen conversion in the liquid-phase oxidation: in the remaining oxygen, the content of  $^{18}\text{O}$  increases, while that of  $^{17}\text{O}$  decreases as a function of conversion. The ratios of the

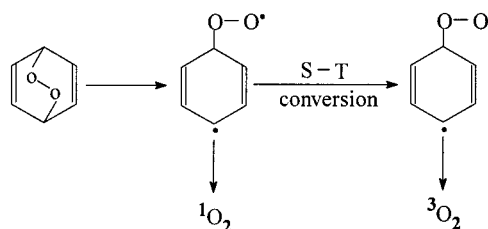
addition rate constants estimated from these dependences are

$$k(^{18}\text{O}^{16}\text{O})/k(^{16}\text{O}^{16}\text{O}) = 0.990 \pm 0.001$$

$$k(^{17}\text{O}^{16}\text{O})/k(^{16}\text{O}^{16}\text{O}) = 1.011 \pm 0.001$$

The former is a measure of CIE, and the latter measures MIE, indicating that  $^{17}\text{O}^{16}\text{O}$  molecules react by 1.1% faster than  $^{16}\text{O}^{16}\text{O}$  molecules. It is worthy to note that in this reaction both effects, CIE and MIE, are quantitatively comparable; usually, MIE strongly dominates over CIE. The reason is hidden, perhaps, in the fast spin relaxation of  $\text{O}_2$  molecule induced by intramolecular dipolar interaction, which does not depend on the nuclear spin and, therefore, induces additional spin conversion which does not affect nuclear spin selectivity.

In 1981, Turro et al.<sup>24</sup> have found  $^{17}\text{O}$  isotope effect in thermal decomposition of endoperoxides, which is believed to occur in the singlet state of the biradical:



The singlet biradical either decomposes to yield singlet oxygen  $^1\text{O}_2$  or undergoes spin conversion into the triplet state and generates triplet  $^3\text{O}_2$ . T-S conversion is faster for biradicals with magnetic  $^{17}\text{O}$  nuclei so that the triplet oxygen is expected to be enriched with  $^{17}\text{O}$ , whereas singlet oxygen  $^1\text{O}_2$  should be depleted with it. This prediction was elegantly confirmed; the magnetic field dependence of the isotope effect has left no doubts in its magnetic nature.

In 1994, a new nuclear spin-selective reaction was found in the high-temperature (350–400 °C) oxidation of aromatic polymers, polypyromellitimide, and polyphenylquinoxaline, by molecular oxygen.<sup>25</sup> At the chemical conversion, 30–65% the remaining oxygen was incremented in  $^{18}\text{O}$  by 0.3–0.6% and depleted in  $^{17}\text{O}$  by 0.4–0.7%.

Kinetic arguments (no autocatalysis in oxygen consumption, no effect of inhibitors on the oxidation rate), as well as composition and yield of reaction products, compel authors to discard the standard chain radical mechanism of oxidation as a source of isotope fractionation. In the proposed mechanism, the key reaction, responsible for chemical and isotope effects, is suggested to be an interaction of low lying and, therefore, thermally accessible excited triplet state of aromatic fragments of macromolecules with molecular oxygen. Spin-selective and isotope-sorting nanoreactor in this case is a pair of two triplets, oxygen and excited fragment. As shown in section 1, only one of the nine spin states in the pair is spin-allowed and generates endoperoxide. The others undergo spin conversion into the singlet state, induced by  $^{17}\text{O}$  hyperfine coupling in molecular oxygen; this process stimulates preferable chemical transformation of  $^{17}\text{O}^{16}\text{O}$  molecules into the endoperoxide and depletes dioxygen by  $^{17}\text{O}$  nuclei.

MIE in this reaction is opposite to CIE; the latter is responsible for the  $^{18}\text{O}$  enrichment (synthesis of endoperoxide from  $^{18}\text{O}^{16}\text{O}$  is slower than that from  $^{16}\text{O}_2$ ); however, MIE markedly dominates over CIE and compensates CIE even in excess.

**C. Silicon-29 MIE.** The first attack on the  $^{29}\text{Si}$  MIE<sup>26</sup> was unsuccessful: photolysis of ketone  $\text{PhCH}_2\text{COSi}(\text{CH}_3)_2\text{Ph}$  was

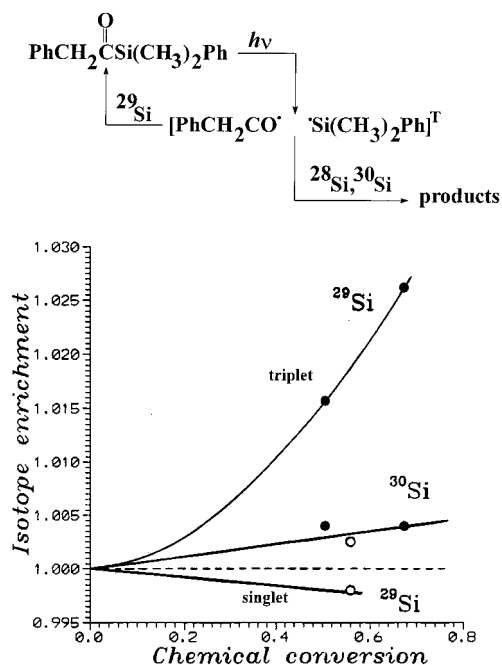


**Figure 6.** Silicon isotope fractionation induced by photolysis of silyl ketone as a function of chemical conversion. CIE-induced fractionation of  $^{30}\text{Si}$  is identical for singlet and triplet channels of photolysis; MIE-induced  $^{29}\text{Si}$  isotope separation depends on the spin multiplicity.

carried out in micelles of Triton X-100, in which radical spin-selective pathway could not compete with spin nonselective reaction channel via siloxycarbenes. However, in 1988 this effect was reliably ascertained in the triplet sensitized photolysis of the same ketone in SDS micelles. The reaction mechanism is shown in Figure 6; it was validated chemically and spectroscopically and confirmed by CIDNP studies.<sup>27</sup> Isotope selection occurs in a triplet radical pair which sorts nuclei in such a way that the magnetic isotope  $^{29}\text{Si}$  is accumulated in the starting, regenerated ketone; nonmagnetic nuclei  $^{28}\text{Si}$  and  $^{30}\text{Si}$  are passed into the reaction products.

MIE clearly dominates over CIE (Figure 6). Moreover, the inversion of the spin multiplicity of radical pair (direct photolysis vs triplet sensitized photolysis) results also in inversion of the MIE: direct photolysis induces impoverishment of the starting ketone by  $^{29}\text{Si}$ ; the effect is smaller than expected for a singlet radical pair as a nuclear spin-sorting nanoreactor. Isotope enrichment of ketone by  $^{30}\text{Si}$ , induced by CIE, does not depend on the spin multiplicity; it perfectly proves the magnetic nature of  $^{29}\text{Si}$  isotope effect.

**D. Sulfur-33 MIE.** The first observation of  $^{33}\text{S}$  MIE was reported by Step, Tarasov, and Buchachenko in 1990:<sup>28</sup> photolysis of sulfur-containing ketone produces triplet radical pairs (Figure 7) which sort isotopic nuclei so that magnetic pairs (with  $^{33}\text{S}$ ) undergo fast T-S conversion and recombine carrying magnetic  $^{33}\text{S}$  nuclei into the starting ketone. Spin conversion of nonmagnetic pairs (with  $^{32}\text{S}$  and  $^{34}\text{S}$ ) is delayed, these pairs predominantly dissociate, and escaped radicals generate the reaction products. The comparison of  $^{33}\text{S}$  and  $^{34}\text{S}$  behavior (Figure 7) demonstrates that MIE is much more efficient in isotope selection than CIE: the one-step enrichment coefficient (see section 3) for  $^{33}\text{S}$  was found to be equal to 1.015; for  $^{34}\text{S}$ , it was 1.008<sup>29</sup>. MIE for  $^{33}\text{S}$  in the same reaction was confirmed by Japanese authors in 1998; they have also detected magnetic field dependence of MIE (see section 5).<sup>30</sup>

**E. Germanium-73 MIE.**  $^{73}\text{Ge}$  MIE was detected first time in 1993<sup>31a</sup>: photolysis of methyltriphenylgermane in Brij35

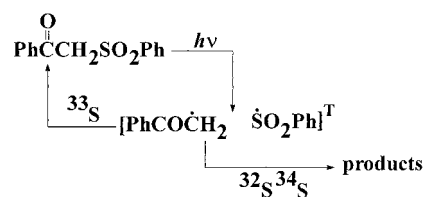


**Figure 7.** Sulfur isotope fractionation induced by photolysis of sulfur-containing ketone as a function of conversion.

micellar solution was suggested to produce a triplet radical pair according to the following scheme:



This pair selects radicals with  $^{73}\text{Ge}$  magnetic nuclei and directs them into the starting molecule so that regenerated  $\text{Ph}_3\text{GeCH}_3$  accumulates  $^{73}\text{Ge}$  nuclei. There were no isotope effect for nonmagnetic  $^{72}\text{Ge}$  nuclei. The pronounced magnetic field dependence on the  $^{73}\text{Ge}$  MIE was also detected. Later, similar MIE was reported for the photolysis of related molecule,  $\text{Ph}_2\text{Ge}(\text{CH}_3)_2$ .<sup>31b</sup>

In specially designed photochemically induced hydrogen atom abstraction reaction of triplet benzophenone with triethylgermane in SDS micelles



A significant enrichment by  $^{73}\text{Ge}$  nuclei of the reaction product, diphenyl(triethylgermyl)methanol, was reported in 1998.<sup>31c</sup> The enrichment was a function of magnetic field, a typical and reliable symptom of MIE; no effect was detected for the nonmagnetic isotope  $^{72}\text{Ge}$  (see section 5).

**F. Uranium-235 MIE.** The uranium-235 MIE was discovered in 1989 and reported in 1990 by Buchachenko, Khudyakov, et al.<sup>32</sup> The search of uranium MIE implies the solution of three problems: (i) to find and to design the reactions of uranium compounds which would generate paramagnetic intermediates, spin carriers; (ii) to identify spin-selective steps in reactions of these intermediates; (iii) to study isotope distribution in the reaction products. The most intriguing and risky problem is the hyperfine coupling constants, since there is no guarantee that the outer unpaired electron is able to reach deeply lying and extremely screened  $^{235}\text{U}$  nucleus and produce an appreciable hyperfine coupling.

Among many reactions of uranium compounds, the photoreduction of the uranyl salts was chosen. A long way to this choice and arguments in its favor are summarized by Buchachenko and Khudyakov.<sup>33</sup> The decisive argument was the spin multi-

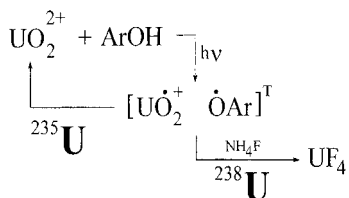


**Figure 8.** Scheme of the MIE-induced uranium isotope fractionation.

plicity of excited uranyl ion  $\text{UO}_2^{2+}$ , which was proved by magnetic field effect and CIDNP to be a triplet.<sup>34</sup>

The photoinduced reaction of uranyl ion with phenols is shown schematically in Figure 8. Spin-selective nanoreactor is a triplet ion–radical pair with uranyl  $\text{UO}_2^+$  ion and phenoxyl as partners. Hyperfine coupling with magnetic  $^{235}\text{U}$  nucleus stimulates T–S conversion of the pair; being in singlet state, it disproportionates the regenerating starting ion  $\text{UO}_2^{2+}$ , which accumulates the  $^{235}\text{U}$  nuclei. The pairs with nonmagnetic  $^{238}\text{U}$  nuclei preferably dissociate in water solution; escaped  $\text{UO}_2^+$  ions disproportionate into  $\text{U}^{4+}$  ions which react with  $\text{NH}_4\text{F}$  and precipitate as an insoluble  $\text{UF}_4$ .

In the first experiments uranyl nitrate and *p*-methoxyphenol were used as reagents; the reaction product,  $\text{UF}_4$ , was depleted by magnetic  $^{235}\text{U}$  nuclei by 0.5% with respect to the starting uranyl. The larger effect was found later by Khudyakov and Buchachenko<sup>35</sup> in the photolysis of uranyl perchlorate in the presence of 2,6-diphenyl-4-stearoyl phenol in SDS micelles. The enrichment of the starting uranyl salt by  $^{235}\text{U}$  and depletion of  $\text{UF}_4$  by this isotope were perfectly balanced.

It is noteworthy that the observed effect is unusual, anticlassical isotope effect; in contrast to CIE, which dictates a higher chemical reactivity of heavy-atom molecules, in the case under study, these molecules are more reactive and decay faster. It means that MIE and CIE for  $^{235}\text{U}$  are of opposite signs; the reason is that in this particular case magnetic nucleus  $^{235}\text{U}$  is lighter than the nonmagnetic  $^{238}\text{U}$ .

Uranium MIE was confirmed in 1992 by Rykov et al. in the photolysis of uranyl succinate in methanol:<sup>36</sup> at the 90% conversion, the enrichment of the starting salt by  $^{235}\text{U}$  reached 6%.

Photoreduction of uranyl salts is the best up-to-date reaction for isotope fractionation via MIE, although it is not perfect because some harmful factors operate in this reaction (such as isotope exchange between reagents and products which results in scrambling of isotopes; for details of the reaction mechanism, physics, and chemistry of uranyl and uranyl ions, see ref 34). These factors prevent the possibility to exhibit the highest MIE-induced isotope fractionation. Nevertheless, MIE in this reaction is remarkable in three aspects:

- (i) Despite the many counteracting factors, MIE-induced isotope fractionation in this reaction is significant, and it exceeds the CIE-induced separation by a ln order of magnitude.
- (ii) It demonstrates that the magnetic electron relaxation in paramagnetic ion  $\text{UO}_2^+$  is rather slow; at least the relaxation time is longer than the time of spin conversion, so the misgiving of large spin–orbital coupling in the heavy atom-centered radical is exaggerated. This coupling appears to be not too strong in order to destroy spin evolution of the pair.
- (iii) Hyperfine coupling in the  $\text{UO}_2^+$  ion is unknown; however, it is large enough to control spin conversion of the radical pair and to produce nuclear spin selection.

**G. MIE: Quantity.** Figure 9 summarizes one-step enrichment coefficients  $\alpha$  which characterize the efficiency of isotope sorting induced by MIE and CIE. It clearly demonstrates the

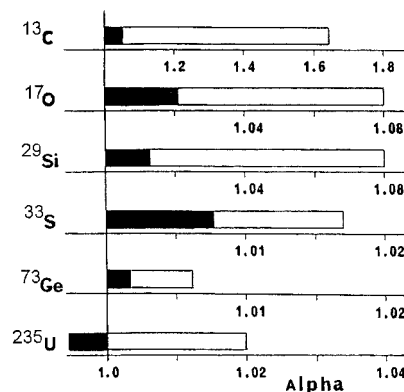
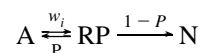


**Figure 9.** One-step enrichment coefficients  $\alpha$ . The red fields indicate the range of  $\alpha$  values of MIE; black fields characterize CIE-induced isotope separation.

advantage of MIE over CIE for all nuclei exhibiting MIE and inspires the further race for the MIE on the other nuclei.

### 3. MIE: Kinetics and Quantitative Parameters

Partly reversible reactions, like DBK photolysis, are the most favorable candidates for the MIE-induced isotope fractionation; in this case, only the starting reactant accumulates magnetic nuclei. The kinetic scheme of such reactions is very simple:



It implies a generation of radical pair RP from the reactant A with the rate  $w_i$  followed by regeneration of A or irreversible transformation into the reaction product N. The same is valid for the molecule  $\text{A}^*$  differing from A only by isotope substitution:



Note that in these schemes the rate of generation of the radical pairs  $w_i$  is supposed to be identical for both isotopic molecules A and  $\text{A}^*$ ; i.e., for the moment, we ignore CIE.

To characterize a system in which both isotopic forms A and  $\text{A}^*$  are presented, the following parameters should be introduced:  $\delta = [\text{A}^*]/[\text{A}]$ , the content of labeled isotope ( $^{13}\text{C}$ , in particular) in the course of reaction;  $\delta_0$  is that at the start of reaction ( $\delta_0 = \delta$  at  $t = 0$ );  $F = ([\text{A}]_0 - [\text{A}])/[\text{A}]_0$  is the chemical conversion of A molecules, and  $F^*$  is that of  $\text{A}^*$  molecules.

A pair of simple kinetic equations describes chemical decay of A and  $\text{A}^*$  molecules:

$$-d[\text{A}]/dt = w_i[\text{A}](1 - P) \quad (2)$$

$$-d[\text{A}^*]/dt = w_i[\text{A}^*](1 - P^*) \quad (3)$$

where  $P$  and  $P^*$  are the recombination probabilities of radicals in RP and  $\text{RP}^*$ , respectively.

The fundamental parameter characterizing isotope separation both in CIE and MIE is a one-step enrichment coefficient  $\alpha$ , i.e., the reduced ratio of the decay rates of A and  $\text{A}^*$  reactants:

$$\alpha = \frac{d[\text{A}]/dt}{w_i[\text{A}]} \left/ \frac{d[\text{A}^*]/dt}{w_i[\text{A}^*]} \right.^{-1} = \frac{1 - P}{1 - P^*} \quad (4)$$

Introducing the very useful parameter  $S = \delta/\delta_0$ , an isotope

enrichment, and going through the kinetic routine, one can derive the following equations:

$$\alpha = \frac{1 - P}{1 - P^*} \quad (5)$$

$$\alpha = \frac{\ln(1 - F)}{\ln(1 - F^*)} \quad (6)$$

$$S = \frac{1 - F^*}{1 - F} \quad (7)$$

which relate the key parameters of MIE –  $P$ ,  $P^*$ , and  $\alpha$  with the kinetic characteristics of reaction –  $F$ ,  $F^*$ , and  $S$ . By the way, it is also not difficult to include into consideration the CIE and derive the equation for the total one-step enrichment coefficient  $\alpha_{\text{tot}}$ :

$$\alpha_{\text{tot}} = \alpha(\text{MIE})\alpha(\text{CIE}) \quad (8)$$

(for details, see ref 37).

If, besides of the back recombination, radical pair exhibits other spin-selective reactions, such as disproportionation, head-to-tail coupling, and electron transfer between radicals (in ion-radical pairs), then magnetic nuclei will be distributed between all products of intrapair reactions, including regenerated starting material. This is not an encouraging situation if one keeps in mind the isotope fractionation and accumulation of magnetic nuclei in a single product; however, it is not a problem to derive the kinetic equations in order to extract parameters of isotope selection even for this complicated situation. It is worthy of mentioning that almost exhausted analysis of possible kinetic situations has been presented by Buchachenko.<sup>19,37</sup>

A scattering of magnetic isotope among many products of intrapair reactions is far from being a desirable situation (for exception, of course, if it is used as a mean to elucidate a mechanism of intra-pair reactions). It would be much more preferable to collect magnetic nuclei in a single product, like in DBK photolysis, but this is a matter of the skill and art of the reaction design. The principles and many beautiful examples of the lucky choice and skillful design of spin-selective reactions were given in section 2.

Concerning experimental methods of studying MIE, one should keep in mind that all of them are those commonly used in CIE studies, with the only addition of NMR spectroscopy to detect magnetic nuclei; for details, see ref 37.

#### 4. MIE: Choreography of Three Dynamics

As a spin-selective nanoreactor any pair of spin carriers is a dynamic system, the partners may leave a pair, execute diffusional motions, random in space, and time, and then return and re-encounter. During these diffusional trips, spin evolution of the pair occurs; to generate a molecule from the triplet (suppose, radical) pair, at least three events in the fate of the pair should be synchronized in space and time.

First, the radicals leaving radical pair (RP) at the moment  $t = 0$  should return and re-encounter at certain instant  $t$ . Depending on the spin state, singlet or triplet, at that time  $t$ , the re-encounter may be successful (molecule is formed) or not; in the latter case, the survived partners repeat a sequence of new diffusional trips and new attempts to react. The key function characterizing this process quantitatively is a molecular dynamic function  $f(t)$ , the probability of the first re-encounter at time  $t$ .

Second, at the moment of re-encounter, when the partners are again in contact, the pair should be in the singlet state in

order to be ready to collapse into the molecule at this moment  $t$ . This process is controlled by spin dynamics; the probability for the RP to appear in singlet state at time  $t$  is determined by coefficient  $|C_s(t)|^2$ , where  $C_s(t)$  is an admixture of singlet component in the total spin wave function of the RP (it will be discussed later).

Third, the RP should be chemically survived to the moment  $t$ ; this process is controlled by chemical dynamics and characterized by function  $\exp(-kt)$ , where  $k$  is the total rate constant of transformation of the pair into the new, secondary pair by radical splitting, scavenging, electron transfer (in ion-radical or electron-hole pairs), etc.

The probability for the molecule to be born from triplet RP at the first re-encounter of partners is expressed by integral

$$P_1^T = \int_0^\infty \epsilon |C_s(t)|^2 f(t) \exp(-kt) dt \quad (9)$$

Here  $\epsilon$  is the cross section of the reaction when partners are in contact and in singlet state—i.e., they are ready to react—and  $\epsilon$  is usually very close to unity.

Thus, the birth of molecule in the intra-pair reaction is a result of collective efforts and coordinated, synchronized in time and space, choreography of three dynamics—spin, molecular and chemical; integral 9 is a central equation to quantitatively estimate a total result of their operation.

**A. Spin Dynamics.** Spin motion in two-electron nanoreactor (for instance, in radical pair) is controlled by magnetic and exchange interactions collected in the spin Hamiltonian:

$$H = \mu_B H_0 (g_1 S_1 + g_2 S_2) + \left[ \sum_i I_i a_i S_1 + \sum_j I_j a_j S_2 \right] - J^{1/2} + 2S_1 S_2 \quad (10)$$

The first term refers to Zeeman interaction between magnetic field  $H_0$  and electron spins  $S_1$  and  $S_2$  of the partners; the second one describes Fermi, or hyperfine, coupling (HFC) of the electron spins  $S_1$  and  $S_2$  with nuclear spins  $I_i$  and  $I_j$  of the corresponding partners. The third term denotes exchange interaction between unpaired electrons of the partners.

In general, Zeeman and Fermi interactions are tensors, so Hamiltonian 10 can be split into two parts, isotropic and anisotropic. Isotropic part induces spin precession of each electron with different frequencies, resulting in spin oscillation of the RP between spin states, singlet (S) and triplet ( $T_0$ ,  $T_\pm$ ); this process driven by isotropic Zeeman and Fermi interactions can be considered as a coherent dephasing.

The anisotropic part is modulated by random motion of radicals; it is responsible for the paramagnetic relaxation characterized by two well-known times  $T_1$  and  $T_2$ :

$$T_i^{-1} = \gamma^2 V^2 \tau (1 + \omega^2 \tau^2)^{-1} \quad (11)$$

where  $V$  is the energy of interactions responsible for the relaxation,<sup>21</sup>  $\omega$  is the energy splitting of electron Zeeman levels, and  $\tau$  is the correlation time of motions modulating magnetic interactions responsible for the relaxation. This contribution can be considered as a stochastic spin conversion (see Figure 10, where the total scheme of the triplet–singlet conversion of the pair is presented).

Neither  $T_1$  nor  $T_2$  separately can induce triplet–singlet conversion of the pair, but in cooperation, stochastic relaxation via  $T_1$  and  $T_2$  results in T–S spin conversion. This mechanism was first proposed by Brochlehurst;<sup>38</sup> however,  $T_1$  and  $T_2$  in nonviscous solutions are estimated for usual light atom-centered

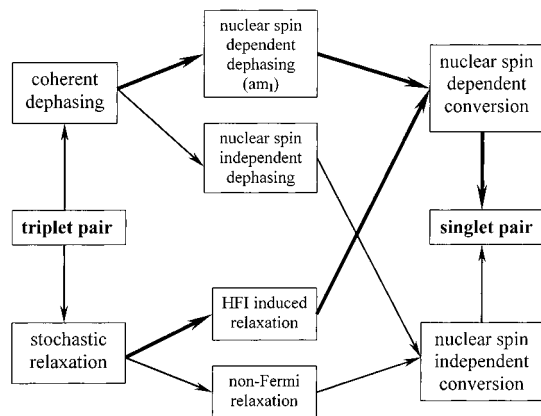


**Figure 10.** Schematic presentation of magnetic interactions characterizing dephasing and stochastic relaxation and their contribution into the nuclear spin selectivity. The thick arrows trace the routes of magnetic nuclei.

radicals to be  $10^{-6}$  to  $10^{-5}$ s, so the relaxation contribution into the spin conversion may be ignored. However, in viscous solutions, in micelles, and in polymers, the relaxation times may be shorter and fall into the range  $10^{-10}$  to  $10^{-7}$ s, commensurable with those of dephasing. Then both mechanisms, dephasing and stochastic relaxation, may contribute on a par into the spin conversion of the pair.

Spin dephasing is controlled by two contributions induced by Fermi (isotropic part of hyperfine coupling) and non-Fermi ( $\Delta g\beta H$  and  $J$ ) interactions, respectively. The former is nuclear spin-dependent and produces isotope selection; the latter does not depend on the nuclear spins (Figure 10). Similarly, stochastic relaxation contributes into two channels of spin conversion, induced by Fermi (anisotropic part of hyperfine coupling) and non-Fermi (anisotropy of  $g$ -factor, dipolar, spin-rotational and spin-orbital coupling) interactions, respectively (Figure 10).

The total triplet-singlet conversion of the radical pair is composed of two parts: the first originates from Fermi interactions, both coherent dephasing and stochastic relaxation; the second is induced by non-Fermi interactions, no matter if they are coherent or stochastic. The former is nuclear spin-dependent—it induces magnetic isotope effect and isotope fractionation—and the latter does not depend on the nuclear spins (Figure 10).

The splitting of spin Hamiltonian (10) into two parts— isotropic, permanently driving spin conversion by coherent dephasing, and anisotropic, time dependent, leading stochastic spin conversion—is the first step in the hierarchy of theories treating spin motion dynamics. The second point in the classification is the exchange interaction. Being a function of inter-radical distance  $r$

$$J(r) = J_0 \exp(-\alpha r) \quad (12)$$

it is modulated by molecular dynamics, so spin dynamics, being a function of exchange potential, are directly related to the molecular dynamics. However,  $J(r)$  is a short-range potential rapidly decreasing at the separation of radicals by one or two molecular diameters, so it operates only in very short diffusional trajectories of radical trips. Their times are very short, significantly shorter than those of spin conversion, so these short trajectories contribute almost nothing into the nuclear spin selection. The main contribution in MIE comes from the long and prolonged trajectories in which exchange interaction is negligible. For this reason, one can neglect the effect of

exchange interaction on spin motion in radical pair during the diffusional trips of radicals between re-encounters and treat spin and molecular dynamics independently.

In this simplifying but physically justified approximation, spin oscillations between singlet and triplet states of the radical pair may be evaluated by solving the time-dependent Schrödinger equation

$$i \frac{\partial \varphi}{\partial t} = H \varphi \quad (13)$$

with the well-known spin wave functions  $|S\rangle$ ,  $|T_0\rangle$ , and  $|T_{\pm}\rangle$  of singlet and triplet states and spin Hamiltonian  $H$ , which includes only isotropic Zeeman and Fermi interactions. The central result of the solution is the probability for the initially triplet pair to be in singlet state at time  $t$

$$|C_{S,rs}^T(t)|^2 = \sin^2 \omega_{12} t \quad (14)$$

where  $\omega_{12}$  are matrix elements of spin Hamiltonian for the triplet-singlet mixing. They are

$$\omega_{12}(T_0) = \langle ^1/2 | (g_1 - g_2)\beta H + \left( \sum_{i,1} a_i m_i^{(1)} - \sum_{i,2} a_i m_i^{(2)} \right) | \quad (15)$$

$$\omega_{12}(T_+) = - \langle ^1/8 | ^{1/2} a_i [I_i(I_i + 1) - m_i(m_i - 1)] \quad (16)$$

$$\omega_{12}(T_-) = \langle ^1/8 | ^{1/2} a_i [I_i(I_i + 1) - m_i(m_i + 1)] \quad (17)$$

for the pairs starting their spin evolution into the singlet state from  $T_0$ ,  $T_+$ , and  $T_-$  states, respectively.

For the  $T_0$ -S transitions, the frequency of spin oscillation is determined by the rate of dephasing, which consists of two terms: the first is the difference of Zeeman energies  $\Delta g\beta H$  of the radical partners 1 and 2,  $\Delta g = g_1 - g_2$ ; the second term is the difference of the total Fermi energies of the partners, where  $a_i$  are HFC constants for all  $i$  sorts of nuclei in radicals 1 and 2.

By combining terms of eq 15 as

$$\omega_{12}(T_0) = \langle ^1/2 | [(g_1\beta H + \sum_i a_i m_i^{(1)}) - (g_2\beta H + \sum_i a_i m_i^{(2)})] \quad (18)$$

one can see that the frequency of  $T_0$ -S conversion is indeed the difference in frequencies of precession of spins on the partners 1 and 2. Schematically, the  $T_0$ -S conversion is shown in Figure 11a. At  $t = 0$ , the phase shift between two precessing spins is zero; however, after time  $\tau_{\text{deph}}$  such as

$$\tau_{\text{deph}} = [(g_1\beta H + \sum_i a_i m_i^{(1)}) - (g_2\beta H + \sum_i a_i m_i^{(2)})]^{-1} \quad (19)$$

the shift reaches  $\pi$ . Now the pair is in singlet state in which electron spins of the partners compensate each other. Dephasing time  $\tau_{\text{deph}}$  is the characteristic time of  $T_0$ -S spin conversion. It is also clear that the rates of dephasing for the magnetic and nonmagnetic pairs are different; it is a source of MIE induced by  $T_0$ -S spin conversion.

$T_{\pm}$ -S transitions are important only in low magnetic fields in which  $T_{\pm}$  and S states are degenerated; in high fields,  $T_{\pm}$  states are switched off by Zeeman splitting and not efficient in spin conversion by dephasing. For  $T_{\pm}$ -S transitions, the precession in strongly coupled electron-nuclear system occurs around the total electron-nuclear spin vector. Dephasing proceeds as shown in Figure 11b: electron-nuclear precession



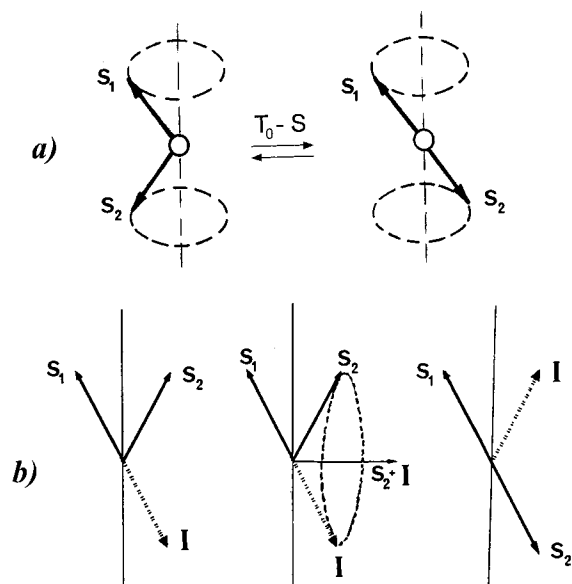


**Figure 11.** Vector presentation of the  $T_0$ -S spin conversion (a) and  $T_+$ -S conversion (b).  $S_1$  and  $S_2$  are electron spins, and  $I$  is a nuclear spin. Spins  $S_2$  and  $I$ , coupled by hyperfine interaction, precess around the total vector  $S_2 + I$  and interchange their orientations in such a way that the  $T_+$  state converts into the S state.

results in exchange of orientations of electron and nuclear spin; the change of electron spin is compensated by that of nuclear spin. The rate of dephasing is determined by eqs 16 and 17, in which  $m_i$  is the nuclear spin projection. The corresponding times of  $T_{\pm}$ -S dephasing are  $[\omega_{12}(T_{\pm})]^{-1}$ ; they depend on the nuclear spin  $I_i$  and HFC constants  $a_i$ , so they are different for magnetic and nonmagnetic pairs; this is another source of MIE induced by  $T_{\pm}$ -S spin conversion which operates only in low magnetic fields.

According to eqs 15–17, the rate of dephasing is a function of  $m_i$ ; for the multinuclear pairs, it is necessary to compute the rate of dephasing for many nuclear spin states differing in  $m_i$  and  $a_i$  and then to average result over  $m_i$  and  $a_i$ . To escape this rather tedious procedure, Schulten et al.<sup>39</sup> have introduced an effective nuclear spin resulting from a quasicontinuous distribution of many nuclear spin orientations. In this approximation, the average HFC constant  $\langle a \rangle$  is combined from the individual  $a_i$ 's of each radical as

$$\langle a \rangle = [(\frac{1}{d}) \sum_i a_i^2 I_i(I_i + 1)]^{1/2} \quad (20)$$

The characteristic times of dephasing vary over the range  $10^{-10}$  to  $10^{-7}$ s, depending on  $g$ -factors and HFC constants  $a$ . From one side, they are too long in comparison with duration of a single collision of reactants in gas-phase reaction,  $\sim 10^{-12}$ s; moreover, in gas reactions, there are no spin correlated re-encounters. This is a reason there are usually no spin and magnetic effects in these reactions. On the other side, the dephasing times are shorter than the typical relaxation times of radicals, both  $T_1$  and  $T_2$  ( $\sim 10^{-6}$ s). Thus, paramagnetic relaxation and, therefore, stochastic spin conversion is by 2–3 orders of magnitude slower than dephasing.

However, in high magnetic fields, such as  $H \geq a$ , the rate of dephasing for spin transitions  $T_{\pm}$ -S decreases and becomes comparable or even less than the rate of stochastic spin conversion. The latter is also important for the radicals with the short  $T_1$  and  $T_2$ , such as  $\bullet\text{OH}$  or metal-centered radicals with

large anisotropy of  $g$ -factors and HFC constants. For these particular cases, stochastic spin conversion competes with or even dominates over dephasing. As a rule, the anisotropy of  $a$  is higher for magnetic nuclei with higher magnetic moments so that even if the stochastic spin conversion dominates, it favors MIE and produces nuclear spin selection.

To take into account an exchange interaction, it is necessary to treat jointly spin and molecular dynamics. It is very easy to do if  $J = \text{constant}$ , but generally, this is not a realistic case (for exception of biradicals or other chemically linked radical pairs but even in these system the approximation  $J = \text{constant}$  is not good enough). The best way for a combined treatment of spin and molecular dynamics as well as spin-dependent reaction kinetics is offered by a stochastic Liouville equation (SLE). It includes the appropriate ensemble average over all the diffusional trajectories; it takes into account how they modulate  $J(r)$  and spin dynamics, both dephasing and stochastic relaxation.

The SLE has been widely exploited by many authors to analyze spin dynamics in magnetic resonance and spin chemistry; historical and hierarchical progress in solving SLE for different purposes has been reviewed in detail by Steiner and Ulrich.<sup>3c</sup> A disadvantage of the SLE solutions is that the results have to be cast in numerical tables; they are sensitive to many parameters, some of which are uncertain, so for any new case, a new solution of SLE is required. Nevertheless, a combination of nonempirical SLE theory and semiempirical treatment based on physical knowledge and intuition provides a complete understanding and satisfactory quantitative description of spin dynamics in chemical reactions of any spin carriers.

**B. Molecular Dynamics.** The molecular dynamic function  $f(t)$  describes the time distribution of diffusional trajectories of radicals. Every re-encounter with probability  $f(t)$  probes spin multiplicity of the pair at time  $t$  and eliminates its singlet character, so the pair being survived after this event behaves like a pair with initial triplet state and starts a new series of re-encounters.

The exponential form of  $f(t) \approx \exp(-\beta t)$ , where  $\beta$  is an empirical kinetic decay parameter of the pair was suggested at the start of spin chemistry; however, the awareness has come shortly thereafter that it is generally not realistic. Adrian was the first who has ingeniously introduced in spin chemistry the Noyes' random flight model with a modified, abridged function  $f(t) = mt^{-3/2}$  which neglects the shortest diffusional trajectories. The complete form of Noyes function

$$f(t)_N = mt^{-3/2} \exp(-\pi m^2/\rho^2 t) \quad (21)$$

has been used by Kaptein<sup>40</sup> and Buchachenko et al.<sup>41</sup> to calculate CIDNP intensities. Here  $\rho$  and  $m$  are defined by

$$\rho = \int_0^\infty f(t) dt \approx 1 - (\frac{1}{2} + \frac{3a}{2d})^{-1} \quad (22)$$

$$m = 1.036(1 - \rho)^2 (a/d)^2 \tau^{-1/2} \quad (23)$$

$a/d$  is the ratio of the radical encounter diameter to the single-step diffusional displacement, and  $\tau$  is the time of diffusional jumps,  $10^{-11}$  to  $10^{-12}$  s. Since the spin motion on the time scale of  $\tau$  is very small, the exact form of  $f(t)$  at short times has little importance.

Another set of functions  $f(t)$  was derived in terms of continuous-diffusion models. The most correct form of the function  $f(t)$  was derived by Schulten and Schulten by solving Smoluchowski equation with radiation boundary conditions.<sup>42</sup>

Razi Naqvi et al.<sup>43</sup> have critically analyzed different continuous diffusion models and found the exact expression of  $f(t)$ :

$$f(t)_{\text{RN}} = \frac{b}{(pDt)^{1/2}} \left( \frac{d}{r_0} \right) \left\{ \exp[-(r_0-d)^2/4Dt] - B(pDt)^{1/2} \exp[B^2Dt + B(r_0-d)] \operatorname{erfc} \left[ B(Dt)^{1/2} + \frac{r_0-d}{2(Dt)^{1/2}} \right] \right\} \quad (24)$$

where  $r_0$  is the initial separation between the partners,  $d$  is the distance of their closest approach,  $B = (b/d + d^{-1})$ ,  $b = \nu l/4$ ,  $\nu$  is a frequency of diffusional jumps ( $\nu = \tau^{-1}$  in eq 23), and  $l$  is an average length of the jumps in diffusional trips. Experimental testing of  $f(t)_{\text{N}}$  and  $f(t)_{\text{RN}}$  will be discussed in section 5.

For two-dimensional molecular dynamics (spin-selective reactions in thin films, Langmuir–Blodgett layers, on the surface of grains in the interstellar space, etc.), the function  $f(t)$  was derived by Deutch,<sup>44</sup> its remarkable property is the time dependence:  $f(t) \approx t^{-1}$ , instead of  $f(t) \approx t^{-3/2}$  for three-dimensional diffusion. It immediately follows that the re-encounter probabilities are higher and regeneration of molecules is more efficient in systems with two-dimensional molecular dynamics; this fact favors MIE-induced isotope selection.

For the one-dimensional diffusion (in pores, extended channels, etc.), the function behaves as  $f(t) \approx t^{-1/2}$  so that it favors MIE even more effectively. The detailed comparative analysis of  $f(t)$  as a function of dimensionality, subjected particularly to MIE, has recently been presented.<sup>45</sup>

For the molecular dynamics of ion-radical pairs (diffusion in Coulomb potential), various functions  $f(t)$  have also been proposed (see ref 46, for instance). Molecular dynamics in microreactors of confined geometry were analyzed by Sterna et al.<sup>15</sup> and Tarasov et al.<sup>47</sup> A model was proposed where one of the partners is fixed at the center of sphere of radius  $R$ , while the other partner could freely migrate reflecting from inner surface of the sphere. The function  $f(t)$  was derived

$$f(t) = \frac{2Dd}{r_0} \sum_{n=1}^{\infty} \exp(-\lambda_n^2 Dt) \frac{(1 + R^2 \lambda_n^2) \lambda_n}{(R-d)(1 + R^2 \lambda_n^2) - R \sin[\lambda_n(r_0-d)]} \quad (25)$$

where  $\lambda_n$  are the roots of the equation

$$\lambda_n = \tan[\lambda_n(R-d)] \quad (26)$$

As earlier,  $d$  is a distance of the closest approach, and  $r_0$  is the initial distance between the partners of the pair. This function was used to compute MIE in nanoconfined reactors (section 5).

**C. Chemical Dynamics.** Chemical dynamics restrict the lifetime of the radical pair by a function  $\exp(-kt)$  and decreases the contribution of long diffusional trajectories into the spin conversion and isotope sorting; it was introduced in spin chemistry by Buchachenko and Markaryan.<sup>48</sup> Chemical dynamics strongly affect the spin dynamics. For short-living radical pairs, with lifetime  $\tau_{\text{RP}} = k^{-1}$  shorter than the characteristic time of spin conversion  $\omega^{-1}$ , the ratio of encounter probabilities for magnetic and nonmagnetic pairs  $P^*/P$  is proportional to  $(\omega^*/\omega)^2$  where  $\omega^*$  and  $\omega$  are frequencies of dephasing in magnetic and nonmagnetic pairs, defined by eqs 15–17. For long-living pairs, at  $\tau_{\text{RP}} > \omega^{-1}$

$$P^*/P \approx (\omega^*/\omega)^{1/2} \quad (27)$$

It is clear that both dynamics are equally important: in the short-living pairs regeneration of molecules is rather low; however, their nuclear spin selectivity is rather high. In the long-living pairs, regeneration of molecules is higher; however, nuclear spin selectivity is lower than that in the short-living pairs. Thus, the lifetime of radicals in a pair is responsible for the production of regenerated molecules, whereas spin dynamics provide isotope loading of these molecules.

In ion–radical pairs in liquids or in electron–hole pairs in molecular solids, chemical dynamics influence spin dynamics by electron hopping between identical molecules, donors or acceptors. Electron jumping between magnetically equivalent molecules results in random modulation of hyperfine coupling due to random distribution of nuclear spin orientations in molecules, participants of the hopping process. The averaging of hyperfine coupling by hopping increases the time of dephasing and suppresses the nuclear spin selectivity of spin conversion. In the limit of fast hopping, when the rate constant of electron jumps  $k \gg a$ , nuclear spin selectivity may be completely destroyed by hopping.

**D. Extended Spin Dynamics.** Extended spin dynamics imply spin dynamics edited by molecular and chemical dynamics; eq 9 integrates their collective effect. It is a basic equation which allows one to calculate the reaction probabilities and forecast MIE and isotope fractionation with a high reliability for the majority of chemical reactions.

The solution of the eq 9 with the Noyes function  $f(t)_{\text{N}}$  was obtained by den Hollander.<sup>49</sup> The corresponding formulas are rather clumsy, but for the most realistic case (when the rate constant  $k$  is considerably less than the frequency of diffusional jumps,  $k \ll m^2$ ), they are more compact:

$$P_1^{\text{T}} = ({}^1/\rho) \epsilon(y - q_{12}) \quad (28)$$

$$y = 1 - ({}^2m/\rho)(\pi k)^{1/2} \quad (29)$$

$$q_{12} = 1 - ({}^m/\rho)(2\pi)^{1/2} [(k^2 + 4\omega_{12}^2)^{1/2} + k]^{1/2} \quad (30)$$

where  $\omega_{12}$  is given by one of the eqs 15–17, depending on what channel of spin conversion we are interesting in.

A general solution of eq 9 with  $f(t)_{\text{RN}}$  was obtained by Belyakov and Buchachenko;<sup>50</sup> the corresponding analytical formulas are too bulky and given in ref 37. Tarasov et al.<sup>47</sup> have calculated  $P_1^{\text{T}}$  with the function  $f(t)$  for the confined nano reactors (eq 25); the values of  $P_1^{\text{T}}$  are suitable to calculate MIE in micelles, zeolite cavities, etc.

All equations of extended spin dynamics are functions of  $\omega_{12}$ , and they result in reaction probabilities for certain nuclear spin states with nuclear spin projections  $m_i$ . The total reaction probability at the first re-encounter,  $P_1^{\text{T}}$ , should be found by summation over all nuclear spin states of the pair.

Each re-encounter of radicals probes spin multiplicity of the pair withdrawing its singlet share and leaving a triplet share which starts a new cycle of triplet–singlet conversion. The total reaction probability is obtained by summation of  $P_1^{\text{T}}$  over all multiple re-encounters. It results in infinite geometrical series

$$P_{\Sigma} = P_1^{\text{T}} + (p - P_1^{\text{T}})P_1^{\text{T}} + (p - P_1^{\text{T}})^2 P_1^{\text{T}} + \dots = \frac{P_1^{\text{T}}}{1 - p + P_1^{\text{T}}} \quad (31)$$

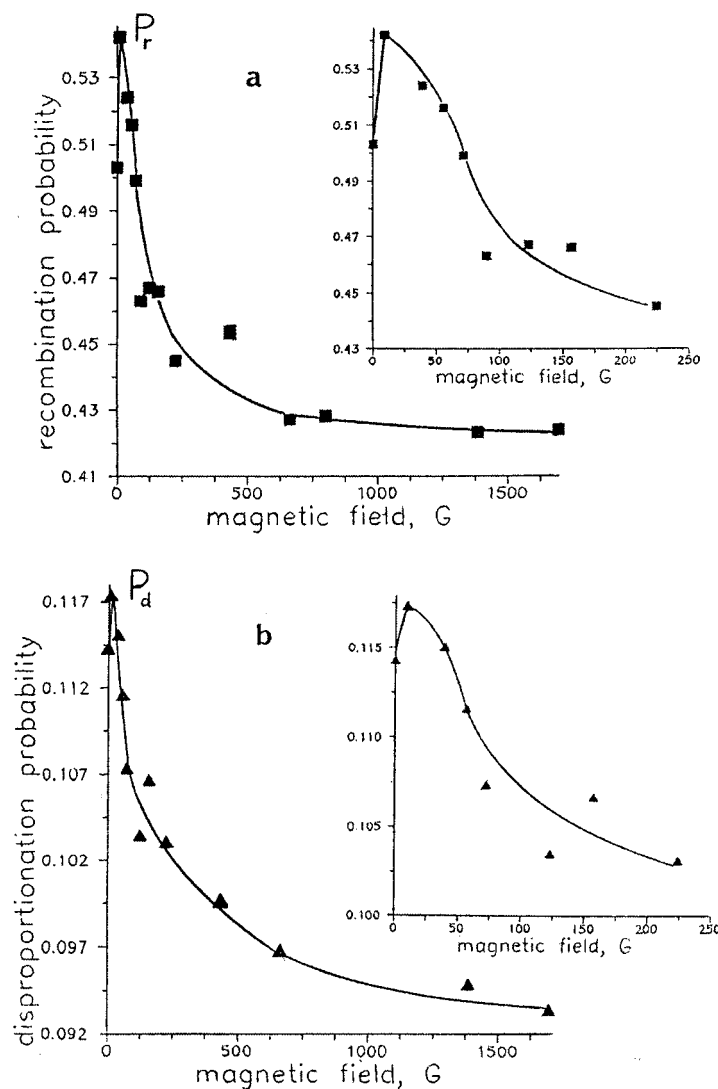


**Figure 12.** Magnetic field dependence of the recombination ( $P_r$ ) and disproportionation ( $P_d$ ) probabilities in the triplet radical pair [Ph  $\dot{C}O$   $\dot{C}H$ -( $CH_3$ )Ph].

where

$$P_1^T = \int_0^\infty \epsilon f(t) \sin^2 \omega_{12} t \exp(-kt) dt \quad (32)$$

$$p = \int_0^\infty \epsilon f(t) \exp(-kt) dt \quad (33)$$

As was mentioned earlier, SLE is frequently exploited by many authors to calculate  $P_\Sigma$ ; many versions of the SLE have been developed for assembling various combinations of different models of spin and molecular dynamics, and they have been fully compiled by Steiner and Ulrich.<sup>3c</sup>

### 5. MIE: Controlling Factors

In contrast to CIE, which responds to chemical structure and reaction mechanism, MIE is a function also of these and of many other factors characterizing spin, molecular, and chemical dynamics, so it is an easily controlled phenomenon. The main manipulated variables are magnetic field, hyperfine coupling, viscosity and diffusion coefficients, temperature, lifetime of radicals, and molecular design of nanoreactors.

**A. Magnetic Field.** The magnetic field sensitivity of MIE was unambiguously demonstrated even in the first, cornerstone

paper<sup>8</sup> on MIE (Figure 3); later, it was confirmed in many other papers. First of all, it was shown that the probabilities of intrapair reactions themselves are magnetic field dependent. As an example, Figure 12 shows the recombination and disproportionation probabilities  $P_r$  and  $P_d$  of the triplet radical pair [PhCO  $\dot{C}H$ ( $CH_3$ )Ph], generated by photolysis of deoxymethylbenzoin, as a function of magnetic field. The decreasing of  $P_r$  and  $P_d$  in high fields is a result of switching off by magnetic field two channels,  $T_\pm$ -S, of triplet-singlet conversion.

However, the most striking effect is an increase of both  $P_r$  and  $P_d$  at very low fields, 10–20G. This effect was shown later to be a universal phenomenon; it originates from the following. In zero magnetic field, all nuclear spin states are degenerated, so all nuclei participate in electron spin conversion as a single nucleus with total, averaged projection. Low magnetic field removes nuclear spin degeneracy, so many nuclear spin states and many channels are now open for the triplet-singlet conversion. As a result, a total rate of spin conversion and, therefore, of the reaction probability increases. This effect operates at low fields,  $\sim(0.1-0.2)a$ ; at higher fields, it is suppressed by electron Zeeman interaction switching off  $T_\pm$ -S channels completely.

According to this idea, an initial rise in the reaction probability at very low fields is expected to be higher for magnetic pairs

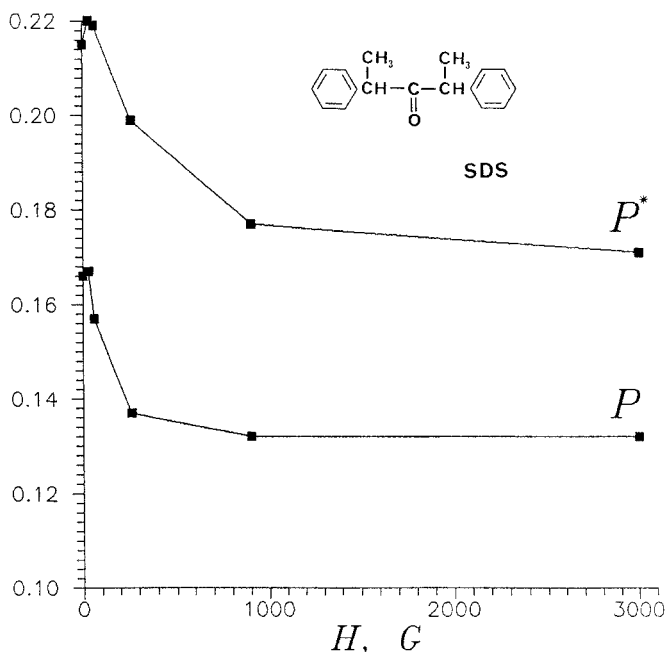


**Figure 13.** Recombination probabilities of magnetic ( $P^*$ ) and non-magnetic ( $P$ ) radical pairs generated by photolysis of diphenylpentanone.

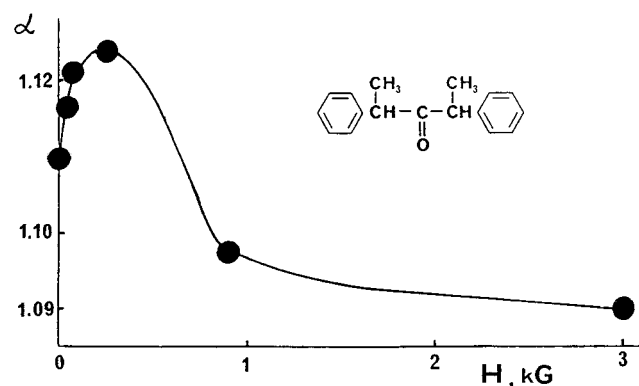


**Figure 14.** Magnetic field dependence of one-step enrichment coefficient in the photolysis of diphenylpentanone.

with respect to that for nonmagnetic pairs because in magnetic pairs the number of magnetic nuclei and nuclear spin states is higher. This forecast works well: Figure 13 demonstrates the recombination probabilities for magnetic ( $^{13}\text{C}$  in carbonyl group) and nonmagnetic triplet pairs [ $\text{PhCH}(\text{CH}_3)\dot{\text{C}}\text{O}\dot{\text{C}}\text{H}(\text{CH}_3)\text{Ph}$ ] generated by photolysis of diphenylpentanone; no doubt, the initial rise for  $P_r^*$  is higher than that for  $P_r$ .

Different sensitivity of  $P_r$  and  $P_r^*$  to the magnetic field results in the maximum for the one-step enrichment coefficient  $\alpha$  as a function of magnetic field (Figure 14). This maximum in low fields is a general property of MIE; Figure 15 demonstrates it for  $^{33}\text{S}$  and  $^{73}\text{Ge}$  MIE.<sup>51</sup>

In high magnetic fields, MIE is strongly suppressed by switching off two of three channels of T-S conversion. However, it is a mistake to suppose that MIE can be completely suppressed by a magnetic field. Only in radical pairs with  $\Delta g \neq 0$  nuclear spin-dependent  $T_0$ -S dephasing may be quenched in very high magnetic fields, when  $\Delta g\beta H \gg a$ , but even in these pairs, stochastic spin conversion remains significant and can produce MIE and isotope selection. For the pairs with  $\Delta g = 0$ , the channel  $T_0$ -S continues to operate via dephasing and stochastic relaxation even in very high fields.

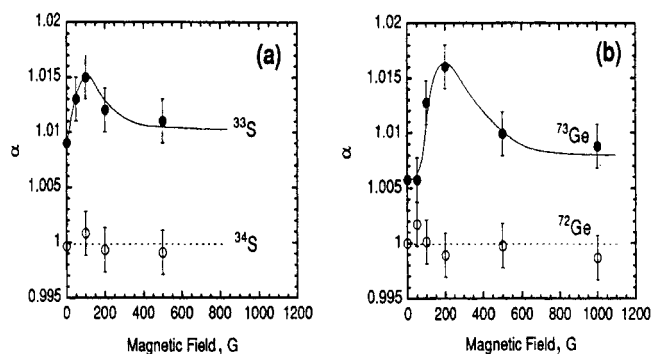
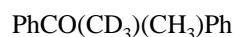


**Figure 15.** Magnetic field dependence of one-step enrichment coefficients of MIE-induced fractionation of sulfur (a) and germanium (b) isotopes.

**B. Hyperfine Coupling.** Being responsible for the nuclear spin selectivity, HFC is the master component among others driving T-S conversion. HFC stimulates recombination of triplet pairs, so  $P^* > P$  (Figure 13). Recombination probabilities of triplet pairs generated by photolysis of chemically identical ketones



increase in this series (0.22, 0.27, 0.30, 0.42) and correlate with HFC energy of the corresponding radical pairs.<sup>52</sup> The decay rate constant of the pair ( $\text{Ph}^{13}\text{CH}_2\cdot \cdot^{13}\text{CH}_2\text{Ph}$ ) generated by laser photolysis of DBK is larger by 50% than that of the pair ( $\text{Ph}^{12}\text{CH}_2\cdot \cdot^{12}\text{CH}_2\text{Ph}$ ).<sup>53</sup> A similar, but inverted effect, was observed by Turro in the emulsion polymerization of styrene, photoinduced by  $\text{Ph}^{13}\text{CH}_2\text{CO}^{13}\text{CH}_2\text{Ph}$  and  $\text{Ph}^{12}\text{CH}_2\text{CO}^{12}\text{CH}_2\text{Ph}$ ; the efficiency of initiation by  $^{13}\text{C}$ -ketone was much lower since the radical pair ( $\text{Ph}^{13}\text{CH}_2\cdot \cdot^{13}\text{CH}_2\text{Ph}$ ) preferably recombines resulting in low yield of polymer.<sup>54</sup>

One-step enrichment coefficients  $\alpha$  are directly related to the HFC; impressive result is shown in Figure 16: in a series of ketones 1-6

$\text{PhCH}_2\text{COCH}_2\text{Ph}$	1
$\text{Ph}^{13}\text{CH}_2\text{COCH}_2\text{Ph}$	2
$\text{PhCH}_2^{13}\text{COCH}_2\text{Ph}$	3
$\text{Ph}^{13}\text{CH}_2^{13}\text{COCH}_2\text{Ph}$	4
$\text{Ph}^{13}\text{CH}_2\text{CO}^{13}\text{CH}_2\text{Ph}$	5
$\text{Ph}^{13}\text{CH}_2^{13}\text{CO}^{13}\text{CH}_2\text{Ph}$	6

$\alpha$  increases as the total HFC energy of the related radical pairs increases. The real message of this result is the conclusion that the most favorable reactions for isotope enrichment are those involving  $\sigma$ -electron radicals in which  $^{13}\text{C}$  HFC constants are large. These are, for example,  $\text{RCO}$  (120G),  $\text{C}_6\text{H}_5$  (150G),  $\text{RC}\equiv\text{C}$  (330G),  $\text{CH}_2\dot{\text{C}}\text{H}$  (108G),  $\dot{\text{C}}\text{N}$  (210G),  $\dot{\text{F}}\text{CO}$  (290G),  $\dot{\text{C}}\text{F}_3$  (270G), and adamantyl (132G). Especially advantageous are

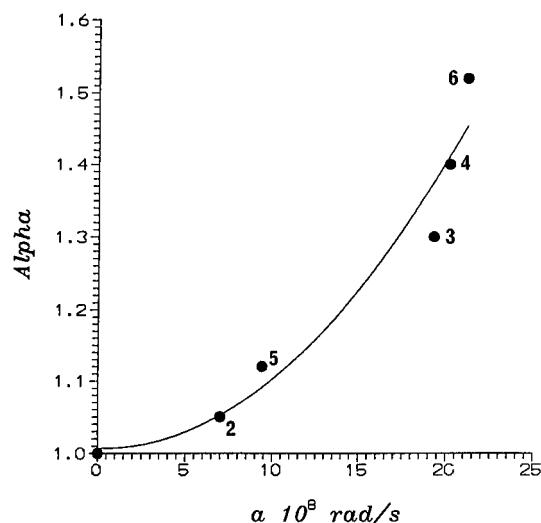


**Figure 16.** One-step enrichment coefficient  $\alpha$  as a function of hyperfine coupling in radical pairs generated by DBK photolysis.

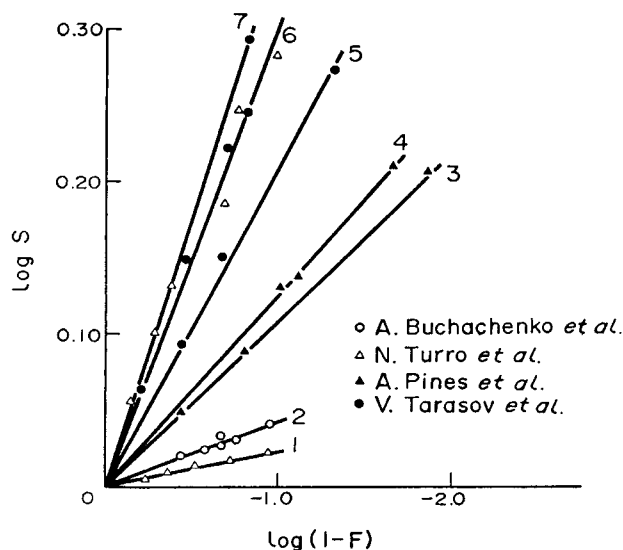


**Figure 17.**  $^{13}\text{C}$  isotope enrichment  $S$  as a function of chemical conversion  $1 - F$  for the DBK photolysis in benzene (1), hexane (2), cyclohexanol at 20 (3) and 0 °C (4), glycerol at 1700 cp (5), micelles (6), and glycerol at 2400 cP (7).

reactions in which both partners are  $\sigma$ -electron radicals and they both contribute into MIE-induced isotope fractionation. A beautiful example is the photolysis of phenyladamantyl ketone AdCOPh; large HFC in the pair ( $\text{Ad}\cdot \cdot \text{COPh}$ ) stimulates (not simultaneously, of course) the recombination of the pair and provides the largest (1.63) known up-to-date one-step enrichment coefficient.<sup>18</sup>

**C. Viscosity and Temperature.** Molecular dynamics do not directly affect the spin dynamics—it is only mediated spin dynamics via modulation of exchange interaction; however, the latter effect has no paramount importance for MIE-induced isotope selection. The main advantage of molecular dynamics is the production of regenerated, isotopically enriched molecules. Figure 17 demonstrates very visually how strong is the dependence of isotope separation on viscosity. The largest efficiency, which even exceeds that observed in micelles by Turro,<sup>13</sup> has been found by Tarasov and Buchachenko<sup>16</sup> in very viscous mixture of glycerol with *tert*-butyl alcohol. It is a striking result that the same reaction, photolysis of dibenzyl ketone, in solutions of varying viscosity exhibits such different

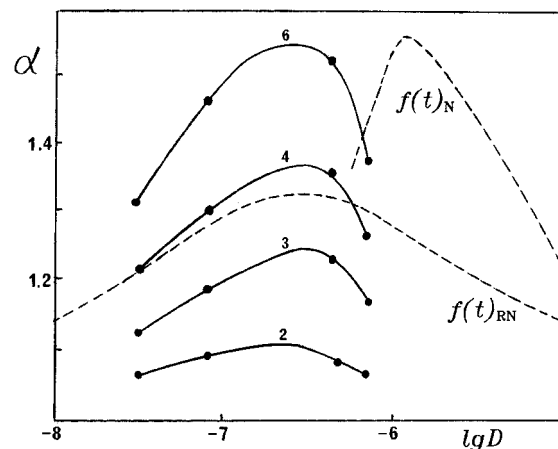


**Figure 18.** One-step enrichment coefficient  $\alpha$  as a function of diffusion coefficient  $D$  for the DBK photolysis in glycerol-*tert*-butanol mixture. The numbers on the curves correspond to those of the DBK isotopic forms 2, 3, 4, and 6. The dotted curves are theoretical dependences calculated with Noyes function  $f(t)_N$  and Razi Naqvi function  $f(t)_{RN}$ .

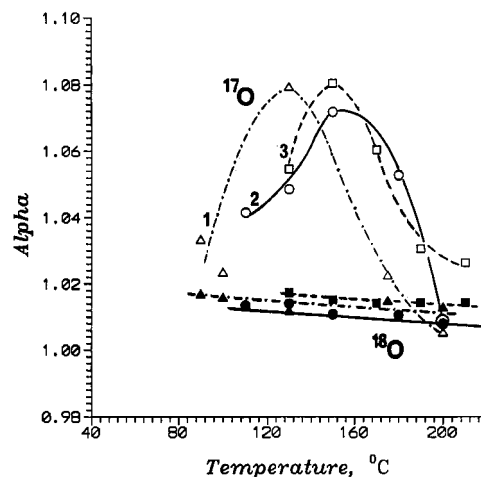


**Figure 19.** Temperature dependence of  $^{17}\text{O}$  and  $^{18}\text{O}$  isotope enrichment in oxidation of polyethylene (1), polypropylene (2), and polymethylpentene (3). Open circles, squares, and triangles correspond to  $^{17}\text{O}$  and the filled symbols to  $^{18}\text{O}$ .

abilities to separate and accumulate isotopes: one-step enrichment coefficients vary over a wide range from 1.03 in benzene to 1.50 in glycerol.

Buchachenko has developed a method of the experimental testing dynamic function  $f(t)$  on the basis of the MIE-induced isotope separation.<sup>55</sup> The experimental functions  $\alpha(\eta)$  for the different isotopic forms 1–6 of DBK, subjected to photolysis in mixtures of glycerol and *tert*-butyl alcohol, have been transformed into the function  $\alpha(\lg D)$ , where  $\eta$  and  $D$  are viscosities and diffusion coefficients; they are shown in Figure 18. The dotted curves are theoretical dependences  $\alpha(\lg D)$  calculated with Noyes function  $f(t)_N$  and Razi Naqvi function  $f(t)_{RN}$  (see section 4). A good agreement with experimental results both in position of maximum and magnitudes of  $\alpha$  is achieved only with the  $f(t)_{RN}$  function. The Noyes function fails to give a quantitative agreement with experiment. This fact seems quite natural because the Noyes flight model is hardly adequate to describe molecular motion in viscous media.

In contrast to CIE, MIE is strongly temperature dependent via diffusion coefficient, the key parameter of the molecular dynamics. Figure 19 demonstrates the impressive distinction in the temperature behavior of  $\alpha$  in the chain oxidation reactions of polymers (section 2): for the CIE-induced  $^{18}\text{O}$  enrichment,

$\alpha$  only slightly depends on temperature, whereas for the MIE-induced  $^{17}\text{O}$  enrichment, the temperature effect is much higher and passes through the maximum, which reflects the most favorable relation of the time scales for molecular and spin dynamics. The proximity of the diffusional lifetime of the peroxy radical pair and the time of its T–S conversion provides the best nuclear spin selectivity. For the short-living diffusional pairs (at high temperatures), T–S conversion has no enough time to produce isotope sorting; for the long-living pairs (at low temperatures), MIE-induced nuclear spin sorting is scrambled.

Molecular dynamics are important to such an extent that it is able even to change the priority of spin-selective reactions. Thus, as was shown in section 2, in the chain oxidation of solid polymers, the chain termination reaction,  $\text{RO}^*_2 + \text{RO}^*_2$ , dominates in the  $^{17}\text{O}$  isotope selection; however, in liquid-phase oxidation, including polymer oxidation in solutions, another spin-selective reaction, chain propagation via  $\text{R}^* + \text{O}_2 \rightarrow \text{RO}^*_2$ , takes a predominance.<sup>23c</sup>

**D. Lifetime of Radicals.** As shown in section 4, the radical lifetime  $\tau_{\text{R}}$  influences on the MIE in two ways: first, it restricts dephasing time if  $\tau_{\text{R}} < \tau_{\text{deph}}$  and, therefore, reduces the time required for spin conversion; second, it kills long diffusional trajectories and reduces regeneration of isotopically enriched molecules. Both are not in favor of MIE and isotope fractionation. It follows from the theory (section 4) and manifests itself experimentally.

One-step  $^{13}\text{C}$  enrichment coefficients for two ketones,  $\text{PhCH}_2\text{-COCH}_2\text{Ph}$  and  $\text{PhCH}(\text{CH}_3)\text{COCH}(\text{CH}_3)\text{Ph}$ , subjected to photolysis in completely identical conditions (SDS micelles,  $20^\circ$ ), are different (1.105 and 1.062 respectively), although  $^{13}\text{C}$  HFC constants in acyl radicals of both ketones are equal, so the spin dynamics of the radical pairs are identical. The only difference is the decarbonylation lifetime of acyl radicals: 75 ns for  $\text{PhCH}_2\text{-CO}$  and 22 ns for  $\text{PhCH}(\text{CH}_3)\text{CO}$ . The shortening in the time of spin evolution results in a significant depressing of MIE. Turro<sup>20</sup> has studied photolysis of DBK in micelles as a function of temperature and shown that one-step enrichment coefficient  $\alpha$  decreases as temperature increases (from 1.4 at  $5^\circ$  to 1.1 at  $70^\circ\text{C}$ ); this result is certainly due to the shortening of the acyl radical lifetime.

**E. Nanoreactors as Nuclear Spin-Selective Devices.** Each cycle of spin-selective cascade (generation of the radical pair, spin conversion, regeneration of the starting molecule) increases isotopic contents in surviving molecules; the most powerful way to stimulate this cascade process is to lock a reaction in a nanoreactor of confined geometry such as micelles, zeolite or porous glass cavities, interlamellar regions of crystalline polymers, two-dimensional pillar structures, etc. Radical pairs prisoned in such a trap are urged to multiply regenerate isotopically enriched molecules. For instance, the recombination probability of the triplet radical pair, generated by photolysis of methyldeoxybenzoin in benzene, was shown to be negligibly small, no more than 0.01; however, for the same pair locked in sodium dodecyl sulfate micelles, this probability is more than 50 times higher.<sup>56</sup>

The strategy of nanoreactors as nuclear spin-selective supramolecular devices was perfectly implemented in photochemically induced MIE in micelles and networks formed by hydrogen bonds in glycerol (section 5c). However, the cascade is a necessary but not sufficient factor to guarantee an efficient isotope selection. Another factor, a ratio  $P^*/P$  which differentiates magnetic and nonmagnetic pairs, is controlled by competition of spin and molecular dynamics of the radical pair in nanoreactor. If spin dynamics are slow and limit the rate of the

RP recombination, the difference in  $P^*$  and  $P$  is large; however, if spin dynamics are fast, the recombination is controlled by diffusional re-encounters of the RP partners in nanoreactor. In this case, magnetically different RP lose substantially their magnetic identity so that the probabilities  $P^*$  and  $P$  tend toward equalizing.

Quantitative criterion of these two dynamic regimes is the relation between the time interval  $\tau_{\text{re}}$  between re-encounters and the time of spin conversion  $\tau_{\text{sc}}$ . The former can be estimated on the pure geometrical reasoning as

$$\tau_{\text{re}} \approx L^2/D \quad (34)$$

where  $L$  is diameter of nanoreactor and  $D$  is the total diffusion coefficient of the partners; the latter is controlled by spin dynamics with characteristic times  $\tau_{\text{sc}}^*$  and  $\tau_{\text{sc}}$  for magnetic and nonmagnetic pairs, respectively.

The relation

$$\tau_{\text{sc}}^* \ll \tau_{\text{sc}} \quad (35)$$

is expected to ensure the most efficient isotope sorting; it implies that recombination of magnetic pairs is controlled by spin dynamics, whereas renaissance of nonmagnetic molecules is governed by molecular dynamics.

This strategy has been successfully tested in the photolysis of methyldeoxybenzoin (both magnetic, labeled  $^{13}\text{C}$  in carbonyl position, and nonmagnetic) in alkyl sulfate micelles of varying size, with alkyl groups from  $\text{C}_8$  to  $\text{C}_{12}$ .<sup>57</sup>

The important conclusion derived from these experiments is that in nanoreactors the exchange interaction between the partners cannot be neglected; spatially restricted diffusion of the partners modulates the exchange potential and suppresses the contribution of hyperfine coupling in spin dephasing. As a result, absolute magnitudes of  $P_{\text{r}}$  and  $P_{\text{r}}^*$  decrease as the size of nanoreactor decreases.

The possible ways to overcome the problems of spin selectivity in nanosized devices including biradicals are discussed in details.<sup>58</sup> Biradicals whose radical centers are linked by flexible chain are very promising systems for isotope selection; they are also flexible with respect to many factors controlling nuclear spin selectivity (inter-radical distances, frequency of re-encounters of termini, etc.). The resources of nanosized molecular devices in MIE-induced isotope fractionation are far from being exhausted.

**F. Does the Limit of MIE Exist?** CIE-induced isotope selectivity is known to be restricted by the isotope mass ratio; MIE-induced nuclear spin fractionation has no such a restriction and exceeds CIE by one or even 2 orders of magnitude (section 2).

There are many factors regulating and controlling MIE so that the question arises, Is there a limit of MIE-induced isotope selectivity similar to that induced by classical, mass-dependent isotope effect?

According to eq 5, the highest magnitude of one-step enrichment coefficient  $\alpha$  is achieved under conditions  $P = 0$  and  $P^* = 1$ , which implies that only magnetic radical pairs recombine and regenerate molecules, while nonmagnetic pairs only dissociate. Then  $\alpha \rightarrow \infty$  and the relation between isotope enrichment  $S$  and chemical conversion  $F$  (eq 7) is

$$S = (1 - F)^{-1} \quad (36)$$

This regime is equivalent to chemically induced isotope

purification; the routes how to practically implement this regime are discussed in sections 2, 4, and 5.

## 6. MIE as a Tool of Mechanistic Chemistry

Any anomalous isotope distribution in the reaction products, incompatible with that expected from CIE, is an unambiguous indication that MIE operates and that the reaction mechanism includes paramagnetic species and elementary steps with their chemical coupling. As a tool of mechanistic chemistry (as well as geochemistry and biochemistry), MIE is an aristocratic method: it requires a high chemical and physical professional culture, but it is compensated for by reliability of conclusions.

MIE provides an excellent test for identification of the spin multiplicity of the reaction intermediates. An example was mentioned in section 2: a direct and sensitized photolysis of silyl ketone has resulted in  $^{29}\text{Si}$  isotope fractionation, different in magnitude and opposite in sign. It is a direct indication of the inversion of the spin multiplicity in these two regimes of photolysis.<sup>27</sup>

Photolysis of benzoyl peroxide sensitized by triplet acetophenone was shown by Molin et al.<sup>12</sup> to result in enrichment of the reaction product, phenylbenzoate, by  $^{13}\text{C}$ . Spin-selective nanoreactor in this case is a triplet radical pair ( $\text{PhCO}_2\cdot\cdot\text{Ph}$ ) which extracts radicals with  $^{13}\text{C}$  into the recombination product. Thermal decomposition of benzoyl peroxide follows the same mechanism, but it includes a singlet radical pair. Benzene isolated from the reaction mixture was shown by Buchachenko and Pershin to be enriched with  $^{13}\text{C}$  by 1.2% at the chemical conversion  $\sim 80\%$ . It is in contrast to CIE, which is expected should result in isotope impoverishment of benzene. This fact evidences that MIE dominates over CIE even in the singlet radical pair reactions.

At last, MIE offers a unique opportunity to distinguish a competition of two reaction channels, radical and nonradical. For this case, a one-step enrichment coefficient is determined by equation

$$\alpha^* = (1 - \theta P)/(1 - \theta P^*) \quad (37)$$

similar to eq 5, but now it includes parameter  $\theta$ , the share of the radical pathway. For the radical channel, one can theoretically calculate  $\alpha$  and by comparing  $\alpha^*$  and  $\alpha$  to find the parameter  $\theta$ . As an example, one can refer to photolysis of silyl ketone in SDS micelles, sensitized by acetophenone, in which radical route was shown to take only  $1/3$ .<sup>27</sup>

Brocklehurst has inspected MIE as a marker for radical pair reactions and electromagnetic field effects in biology (with especial emphasis to tomography); he concluded that the effects may be small but detectable and are worthy of looking for.<sup>59</sup>

## 7. Microwave Induced MIE

A new powerful strategy to enhance MIE and isotope selection is a microwave-induced MIE (MIMIE). It is a new highlight in spin chemistry, a beautiful way to modify chemical reactivity by spin manipulation using selective, frequency-tuned microwave pumping of the reactive intermediates, such as radical pairs.

The idea of MIMIE was suggested and clearly formulated in 1981<sup>60</sup> and elegantly illustrated experimentally in 1991.<sup>61</sup> It implies that the generation of radicals and radical pairs takes place in magnetic field, say, in the cavity of ESR spectrometer; then the frequency-tuned microwave irradiation induces resonant spin transitions between electron Zeeman levels of radicals.

There exists a great variety of regimes how to manipulate with radical pair spin states by microwaves, i.e., how to pump ESR transitions in radical pair (see,<sup>2</sup> for instance). In general, they can be combined into two groups:

Spin inversion which occurs at low amplitudes of microwave pumping  $\gamma H_1 < a$ , where  $H_1$  is a microwave field. Suppose that there is a triplet radical pair; at high magnetic field,  $T_{\pm}$  states of the pair are distant from  $T_0$  states by Zeeman energy  $g\beta H$  and switched off the triplet–singlet conversion.  $T_0$ –S fast conversion, induced by Zeeman and Fermi interaction, empties  $T_0$  state due to leakage of singlet pairs into the reaction product. Microwave-induced ESR transitions in any radical of the pair stimulate  $T_{\pm}$ – $T_0$  conversion and populate  $T_0$  state, increasing the yield of reaction products.

If chemical reaction generates two sorts of radical pairs, say, magnetic and nonmagnetic (for instance, ( $\text{PhCH}_2\text{CO}\cdot\cdot\text{CH}_2\text{Ph}$ ) and ( $\text{PhCH}_2^{13}\text{CO}\cdot\cdot\text{CH}_2\text{Ph}$ ) in the photolysis of dibenzyl ketone) and their ESR spectra are not overlapped, then one can separately, at different microwave frequencies, induce  $T_{\pm}$ – $T_0$  conversion in magnetic or nonmagnetic pair. The former enhances regeneration of magnetic, isotopically enriched molecules, while the latter increases the yield of nonmagnetic molecules. Thus, the ESR pumping of magnetic pairs enhances efficiency of MIE-induced isotope sorting.

Spin locking regime takes place at high microwave power, when  $\gamma H_1 > a$ ; in contrast to spin inversion, spin locking implies that the ESR transitions occur simultaneously in both radical partners. In other words, microwave magnetic field urges both electron spins to precess coherently, in phase. It prevents spin dephasing and triplet–singlet conversion of the pair; i.e., the pair is locked, it is not able to react, and it only dissociates. To enhance isotope selection in a spin locking regime it would be desirable to lock nonmagnetic pairs to prevent their recombination and regeneration of nonmagnetic (with  $^{12}\text{C}$  nuclei) molecules.

To make available this situation, it is necessary to pump all ESR transitions in nonmagnetic pairs. For instance, in pair ( $\text{PhCH}_2\text{CO}\cdot\cdot\text{CH}_2\text{Ph}$ ) from dibenzyl ketone spin, locking regime is satisfied at  $\gamma H_1 > a_H^{\text{max}}$ , where  $a_H^{\text{max}}$  is the largest hyperfine splitting (46 MHz for  $\text{CH}_2$  protons in benzyl radical). At this condition, the ESR transitions in both radicals of the pair are in phase, so dephasing and T–S transitions are forbidden.

Figure 20 illustrates these arguments quantitatively on the example of the radical pairs from dibenzyl ketone; it shows theoretical one-step enrichment coefficients  $\alpha$  as a function of the microwave power  $H_1$  for two cases: the pumping of magnetic pairs ( $\text{PhCH}_2^{13}\text{CO}\cdot\cdot\text{CH}_2\text{Ph}$ ) (curve 1) and nonmagnetic pairs ( $\text{PhCH}_2\text{CO}\cdot\cdot\text{CH}_2\text{Ph}$ ) (curve 2).

Microwave pumping of magnetic pairs occurs in the regime of spin inversion; it stimulates recombination of magnetic pairs and regeneration of magnetic (with  $^{13}\text{C}$ ) DBK molecules;  $\alpha$  continuously grows as  $H_1$  increases. The spin locking regime for magnetic pairs is not attainable since it requires a very high microwave power  $\gamma H_1 = a(^{13}\text{C})$ , where  $a(^{13}\text{C})$  is hyperfine splitting in  $\text{PhCH}_2^{13}\text{CO}$  radical (350 MHz).

Microwave pumping of nonmagnetic pairs at low  $\gamma H_1$  proceeds in the regime of spin inversion; it stimulates triplet–singlet conversion of the pair, increases the yield of regenerated molecules, and decreases  $\alpha$  (curve 2). However, at higher power of pumping the spin locking regime gradually dominates; it suppresses triplet–singlet conversion and prevents recombination of the pairs and regeneration of the nonmagnetic molecules, resulting in enhancement of isotope enrichment of DBK molecules.

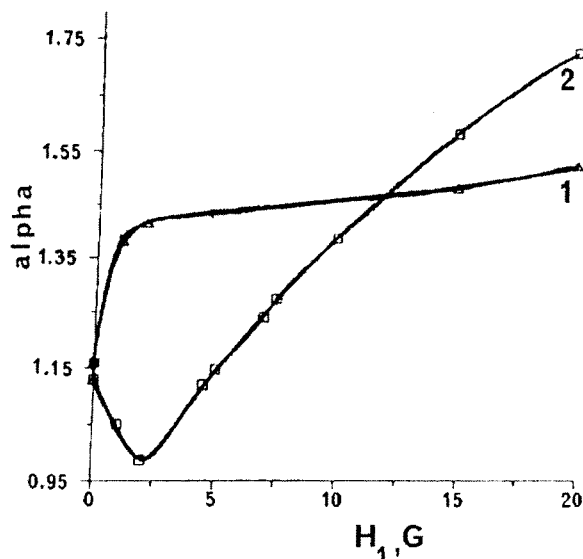


**Figure 20.** Calculated one-step enrichment coefficients  $\alpha$  for  $^{13}\text{C}$  as a function of microwave field  $H_1$  with pumping of magnetic (1) and nonmagnetic (2) radical pairs of phenacyl and benzyl radicals.

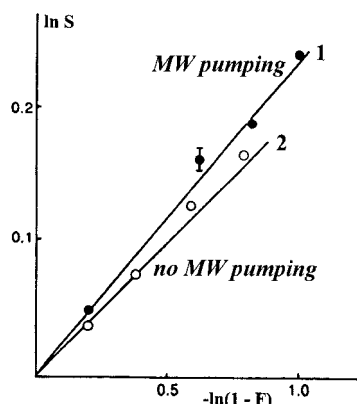


**Figure 21.**  $^{13}\text{C}$  isotope enrichment as a function of chemical conversion in the photolysis of dibenzyl ketone with (1) and without (2) microwave pumping.

The most efficient regime for isotope selection is expected to be simultaneous microwave pumping of both magnetic and nonmagnetic pairs—the former in the regime of spin inversion which stimulates regeneration of molecules with  $^{13}\text{C}$  and the latter in spin locking regime which prevents regeneration of molecules with  $^{12}\text{C}$ . It would result in unlimited isotope fractionation; it is feasible because ESR spectra of magnetic and nonmagnetic pairs are usually not overlapping (at last in the case of DBK), and it can be done in the same ESR-cavity.

Experimentally, only the first regime has been tested:<sup>20</sup> microwave pumping of magnetic pairs ( $\text{PhCH}_2^{13}\text{CO}\cdot\text{CH}_2\text{Ph}$ ) on the high field component of  $^{13}\text{C}$  doublet ( $m = -1/2$ ) in the ESR spectrum of  $\text{PhCH}_2^{13}\text{CO}$  in magnetic field 60.3 mT at  $H_1 = 0.48$  mT was shown to increase  $\alpha$  by 6% (Figure 21). More perfect experiments, at higher  $H_1$ , are expected to give more impressive results.

MIMIE is a beautiful phenomenon which clearly demonstrates how one can selectively modify and control chemical reactivity by microwaves tunable on frequency and amplitude.

## 8. Conclusion

Nuclear mass and nuclear spin selectivity of chemical reactions result in two remarkable phenomena—classical and magnetic isotope effects. However, in contrast to CIE, which

is limited by nuclear mass ratio, MIE has no limit. Furthermore, in contrast to CIE, which is a function of the chemical energy of reactants and transition state only, MIE is easily controllable, compliant to many factors such as hyperfine coupling, magnetic field, magnetic relaxation times, spin multiplicity, viscosity, lifetime of spin carriers, temperature, nanoconfinement of the reactants, and microwave resonant irradiation.

Two facets of MIE manifest themselves very clearly, probing and controlling. The former is a key to mechanistic chemistry, biochemistry, geochemistry, and space chemistry; it is a means to trace long-term chemical evolution of substances in Nature, as well as the origin and chemical evolution of ores, minerals, oils and gas deposits on the Earth. The latter ensures very effective mechanisms of isotope fractionation, isotope enrichment, and accumulation. The key to the control of nuclear spin selectivity is a spin dynamics combined with molecular and chemical dynamics. The problem is not only to ensure a comfort for the spin evolution (strong hyperfine coupling, optimal lifetimes of the spin-selective reaction partners, favorable molecular dynamics). It is even more important to choose spin-selective reaction to direct it through the paramagnetic intermediates in order to create the required pairs of these species, to prepare a favorable starting spin multiplicity of the pairs. It is a matter of the skillful art and science of reaction control. In other words, chemical reaction should be chosen, adapted and designed for the MIE. General principles of the MIE-tuning of the reactions are discussed and illustrated by variety of examples in this paper.

Besides the many factors controlling nuclear spin selectivity, there are two outstanding and highly promising but not yet properly exploited, microwave induced MIE and dimensionality. The former is shortly discussed in section 7, and it carries an unlimited possibilities to enhance nuclear fractionation by microwaves. The latter is based on the strong dependence of the molecular dynamics on the dimensionality: the reactions in two-dimensional layers or in one-dimensional channels are expected to produce very high isotope fractionation. These two ideas are expected to ensure the future breakthroughs in nuclear spin control and magnetic isotope effect.

**Acknowledgment.** Over the years, the author was happy to work with colleagues from the Institute of Chemical Physics—V. F. Tarasov, E. N. Step, I. V. Khudyakov, L. L. Yasina, and I. A. Shkrob. He is grateful to all of them for their fruitful and long-term friendly collaboration. Special gratitude to Prof. N. J. Turro for his inspiring support of the collaboration in MIE between ICP and Columbia University. Financial support of research in spin chemistry and MIE was supplied by Russian Fund of Fundamental Research, Russian Integration Fund and INTAS Project; it is the author's pleasure to acknowledge these Organizations.

## References and Notes

- (1) Zewail, A. H. *J. Phys. Chem. A* **2000**, *104*, 5660.
- (2) Buchachenko, A. L.; Frankevich, E. L. *Chemical Generation and Reception of Radio- and Microwaves*; VCH Publishers: New York, 1993.
- (3) (a) Lepley, A. R.; Closs, G. L. *Chemically Induced Magnetic Polarization*; London; Wiley: New York, 1978. (b) Salikhov, K. M.; Molin, Y. N.; Sagdeev, R. Z.; Buchachenko, A. L. *Spin Polarization and Magnetic Effects in Radical Reactions*; Elsevier: Amsterdam, 1984. (c) Steiner, U.; Ulrich, T. *Chem Rev.* **1989**, *89*, 51. (d) McLauchlan, K. A.; Steiner, U. E. *Mol. Phys.* **1991**, *73*, 241. (e) Buchachenko, A. L. *Pure Appl. Chem.*, in press. (f) Frankevich, E. L.; Kubarev, S. I. In *Triplet State ODMR Spectroscopy*; Clarke, R. H., Ed.; Wiley: New York, 1982; p 138. (g) Buchachenko, A. L.; Berdinsky, V. L. *Russ. Chem. Rev. (Engl. Transl.)* **1983**, *52*, 1. (h) Buchachenko, A. L.; Berdinsky, V. L. *J. Phys. Chem.* **1996**, *100*, 18292.



- (4) Grissom, C. B. *Chem. Rev.* **1995**, 95, 3.
- (5) (a) Hoff, A. J. *J. Photochem. Photobiol.* **1986**, 43, 727. (b) Proskuryakov, I. I.; Klenina, I. B.; Borovykh, I. V.; Gast, P.; Hoff, A. J. *Chem. Phys. Lett.* **1999**, 299, 566.
- (6) Golovin, Y. I.; Morgumov, R. B. *Chem. Rev.* **1998**, 24, 1.
- (7) Buchachenko A. L. *Russ. Chem. Rev. (Engl. Transl.)* **1999**, 68, 85.
- (8) Buchachenko, A. L.; Galimov, E. M.; Nikiforov, G. A. *Dokl. Akad. Nauk SSSR* **1976**, 228, 379.
- (9) (a) Bargon, J.; Fischer, H.; Johnsen, U. *Z. Naturforsch.* **1967**, A22, 1551. (b) Ward, H. R.; Lawler, R. G. *J. Am. Chem. Soc.* **1967**, 89, 5518.
- (10) Lawler, R. G.; Evans, G. T. *Ind. Chim. Belges.* **1971**, 36, 1087.
- (11) (a) Lippmaa, E. T.; Pehk, T. I.; Buchachenko, A. L.; Rykov, S. V. *Dokl. Acad. Nauk SSSR* **1970**, 195, 632. (b) Lippmaa, E. T.; Pehk, T. I.; Buchachenko, A. L.; Rykov, S. V. *Chem. Phys. Lett.* **1970**, 5, 521.
- (12) Sagdeev, R. Z.; Leshina, T. V.; Kamkha, M.; Belchenko, O.; Molin, Yu. N.; Rezvukhin, A. *Chem. Phys. Lett.* **1977**, 48, 89.
- (13) Turro, N. J.; Kraeutler, B. *J. Am. Chem. Soc.* **1978**, 100, 7432.
- (14) (a) Turro, N. J.; Kraeutler, B.; Anderson, D. R. *J. Am. Chem. Soc.* **1979**, 101, 7435. (b) Turro, N. J. *Proc. Natl. Acad. Sci. USA* **1983**, 80, 609.
- (15) Sterna, L.; Ronis, D.; Wolfe, S.; Pines, A. *J. Chem. Phys.* **1980**, 73, 5493.
- (16) Tarasov, V. F.; Buchachenko, A. L. *Izvest. Akad. Nauk SSSR, Ser. Khim.* **1982**, 8, 1927.
- (17) (a) Turro, N. J.; Anderson, D. R.; Chow, M.-f.; Chung, C.-J.; Kraeutler, B. *J. Am. Chem. Soc.* **1981**, 103, 3892. (b) Turro, N. J.; Chung, C.-J.; Lawler, R. G.; Smith, W. J. *Tetrahedron Lett.* **1982**, 23, 3223. (c) Turro, N. J. *J. Am. Chem. Soc.* **1983**, 105, 1572. (c) Turro, N. J. *J. Phys. Chem.* **1985**, 89, 1567.
- (18) Turro, N. J.; Anderson, D. R.; Kraeutler, B. *Tetrahedron Lett.* **1980**, 21, 3.
- (19) Buchachenko, A. L. *Prog. React. Kinet.* **1984**, 13, 164.
- (20) (a) Kraeutler, B.; Turro, N. *J. Chem. Phys. Lett.* **1980**, 70, 270. (b) Turro, N. J.; Chow, M.-F.; Kraeutler, B. *Chem. Phys. Lett.* **1980**, 73, 545.
- (21) Step, E. N.; Tarasov, V. F.; Buchachenko, A. L.; Turro, N. J. *J. Phys. Chem.* **1993**, 97, 363.
- (22) Belyakov, V. A.; Galimov, E. M.; Buchachenko, A. L. *Dokl. Akad. Nauk SSSR* **1978**, 243, 924.
- (23) (a) Buchachenko, A. L.; Yasina, L. L.; Galimov, E. M. *Chem. Phys. Lett.* **1984**, 103, 405. (b) Yasina, L. L.; Buchachenko, A. L. *Chem. Phys.* **1990**, 146, 225. (c) Buchachenko, A. L.; Yasina, L. L.; Belyakov, V. A. *J. Phys. Chem.* **1995**, 99, 4964.
- (24) (a) Turro, N. J.; Weed, G. C. *J. Am. Chem. Soc.* **1983**, 105, 1861. (b) Turro, N. J.; Chow, M.-F.; Rigaudy, J. *J. Am. Chem. Soc.* **1981**, 103, 7218.
- (25) Buchachenko, A. L.; Yasina, L. L.; Vdovina, A. L.; Blumenfeld, A. B. *Russ. Chem. Bull.* **1994**, 43, 1328.
- (26) Step, E. N.; Tarasov, V. F.; Buchachenko, A. L. *J. Gen. Chem. USSR* **1985**, 55, 2348.
- (27) (a) Step, E. N.; Tarasov, V. F.; Buchachenko, A. L.; Ustinov, V. I.; Grinenko, V. A. *Russ. Chem. Bull.* **1988**, 2, 200. (b) Step, E. N.; Tarasov, V. F.; Buchachenko, A. L. *Chem. Phys. Lett.* **1988**, 144, 523.
- (28) Step, E. N.; Tarasov, V. F.; Buchachenko, A. L. *Nature* **1990**, 345, 25.
- (29) Step, E. N.; Buchachenko A. L.; Turro, N. J. *Chem. Phys.* **1992**, 162, 189.
- (30) Wakasa, M. In *Dynamic Spin Chemistry*; Nagakura, S., Hayashi, H., Azumi, T., Eds.; Kodansha, Wiley: Tokyo, 1998, p 37.
- (31) (a) Wakasa, M.; Hayashi, H.; Kobayashi, T.; Takada, T. *J. Phys. Chem.* **1993**, 97, 13444. (b) Wakasa, M.; Hayashi, H.; Ohara, K.; Takada, T. *J. Am. Chem. Soc.* **1998**, 120, 3227. (c) Wakasa, M. In *Dynamic Spin Chemistry*; Nagakura, S., Hayashi, H., Azumi, T., Eds.; Kodansha, Wiley: Tokyo, 1998, p 35.
- (32) (a) Khudyakov, I. V.; Buchachenko, A. L. *Proc. XIV Mendeleev Congress Pure Appl. Chem.* **1989**, 1, 40. (b) Buchachenko, A. L.; Khudyakov, I. V.; Klimchuk, E. S.; Golubkova, N. A. *Russ. Chem. Bull.* **1990**, 9, 1902.
- (33) (a) Buchachenko, A. L.; Khudyakov, I. V. *Acc. Chem. Res.* **1991**, 24, 177. (b) Buchachenko, A. L.; Khudyakov, I. V. *Russ. Chem. Rev.* **1991**, 60, 555.
- (34) (a) Buchachenko, A. L.; Khudyakov, I. V.; Klimchuk, E. S.; Margulis, L. A. *J. Photochem. Photobiol.* **1989**, 46, 281. (b) Golubkova, N.; Khudyakov, I.; Topchiev, D.; Buchachenko, A.L. *Doklady Akad. Nauk SSSR* **1988**, 300, 147.
- (35) Khudyakov, I. V.; Buchachenko, A. L. *Mendeleev Commun.* **1993**, 135.
- (36) Rykov, S. V.; Khudyakov, I. V.; Skakovsky, E. D.; Tychinskaya, L. *J. Photochem. Photobiol., A* **1992**, 66, 127.
- (37) Buchachenko, A. L. *Chem. Rev.* **1995**, 95, 2507.
- (38) Brocklehurst, B. *Radiat. Phys. Chem.* **1983**, 21, 57.
- (39) Schulten, K.; Wolynes, P. *J. Chem. Phys.* **1978**, 68, 3292.
- (40) (a) Kaptein, R. *J. Am. Chem. Soc.* **1972**, 94, 6251. (b) Kaptein, R.; den Hollander, J. A. *J. Am. Chem. Soc.* **1972**, 94, 6269.
- (41) Buchachenko, A. L.; Markaryan, Sh. A. *Org. Magn. Reson.* **1973**, 5, 247.
- (42) Schulten, Z.; Schulten, K. *J. Am. Chem. Phys.* **1977**, 66, 4616.
- (43) Razi Naqvi, K.; Mork, K. J.; Waldenström, S. *J. Phys. Chem.* **1980**, 84, 1315.
- (44) Deutch, J. *J. Chem. Phys.* **1972**, 56, 6076.
- (45) Buchachenko, A. L.; Prostnev, A. S. *Chem. Phys. Lett.*, submitted.
- (46) Buchachenko, A. L. *Chemical Polarization of Electrons and Nuclei*; Science Publ.: Moscow, 1974 (in Russian).
- (47) Tarasov, V. F.; Buchachenko, A. L. *J. Phys. Chem. (Russ.)* **1981**, 55, 1921.
- (48) Buchachenko, A. L.; Markaryan, Sh. A. *React. Kinet. Catal. Lett.* **1974**, 1, 157.
- (49) (a) den Hollander, J. A. *Chem. Phys.* **1975**, 10, 167. (b) den Hollander, J. A. *Chem. Phys. Lett.* **1976**, 41, 257.
- (50) Belyakov, V. A.; Buchachenko, A. L. *Chem. Phys. (Russ.)* **1983**, 10, 1385; *11*, 1510.
- (51) Wakasa, M. In *Dynamic Spin Chemistry*; Nagakura, S., Hayashi, H., Azumi, T., Eds.; Kodansha, Wiley: Tokyo, 1998; p 39.
- (52) Turro, N. J.; Mattay, J. *J. Am. Chem. Soc.* **1981**, 103, 4200.
- (53) Turro, N. J.; Chow, M.-F.; Chung, C.-J.; Tanimoto, Y.; Weed, G. *J. Am. Chem. Soc.* **1981**, 103, 4574.
- (54) (a) Turro, N. J. *J. Am. Chem. Soc.* **1980**, 102, 7391. (b) Turro, N. J.; Chow, M.-F.; Chung, C.-J.; Tung, C.-H. *J. Am. Chem. Soc.* **1983**, 105, 6347.
- (55) Buchachenko, A. L. *Russ. Chem. Bull.* **1995**, 44, 1639.
- (56) Step, E. N.; Buchachenko A. L.; Turro, N. J. *J. Org. Chem.* **1992**, 57, 7018.
- (57) (a) Tarasov, V. F.; Ghatlia, N. D.; Buchachenko, A. L.; Turro, N. J. *J. Am. Chem. Soc.* **1992**, 114, 9517. (b) Tarasov, V. F.; Ghatlia, N. D.; Buchachenko, A. L.; Turro, N. J. *J. Am. Chem. Soc.* **1994**, 116, 2281. (c) Tarasov, V. F.; Ghatlia, N. D.; Buchachenko, A. L.; Turro, N. J. *J. Phys. Chem.* **1991**, 95, 10220. (d) Turro, N. J.; Buchachenko, A. L.; Tarasov, V. F. *Acc. Chem. Res.* **1995**, 28, 69.
- (58) Buchachenko, A. L.; Berdinsky, V. L. *J. Phys. Chem. A* **1999**, 103, 865.
- (59) Brocklehurst, B. *Int. J. Radiat. Biol.* **1997**, 72, 587.
- (60) Buchachenko, A. L.; Tarasov, V. F. *Russ. J. Phys. Chem.* **1981**, 55, 936.
- (61) Tarasov, V. F.; Bagryanskaya, E. G.; Grishin, Y. A.; Sagdeev, R. Z.; Buchachenko, A. L. *Mendeleev Commun.* **1991**, 85.